

Direct interaction of Su(var)2-10 via the SIM-binding site of the Piwi protein is required for transposon silencing in *Drosophila melanogaster*

Melinda Bence¹ , Ferenc Jankovics^{1,2}, Ildikó Kristó¹, Ákos Gyetvai¹, Beáta G. Vértessy^{3,4}  and Miklós Erdélyi¹ 

1 Institute of Genetics, HUN-REN Biological Research Centre, Szeged, Hungary

2 Department of Medical Biology, University of Szeged, Hungary

3 Department of Applied Biotechnology and Food Sciences, Budapest University of Technology and Economics, Hungary

4 Institute of Enzymology, HUN-REN Research Centre of Natural Sciences, Budapest, Hungary

Keywords

Drosophila melanogaster; PIWI/piRNA; Su(var)2-10; sumoylation; transposon silencing

Correspondence

M. Bence and M. Erdélyi, Institute of Genetics, Biological Research Centre, Szeged, Temesvári krt. 62, Szeged H-6726, Hungary

Tel: +36 62 599686; +36 62 599670

E-mail: bence.melinda@brc.hu; erdelyi.miklos@brc.hu

(Received 25 July 2023, revised 30

November 2023, accepted 22 January 2024)

doi:10.1111/febs.17073

Nuclear Piwi/Piwi-interacting RNA complexes mediate co-transcriptional silencing of transposable elements by inducing local heterochromatin formation. In *Drosophila*, sumoylation plays an essential role in the assembly of the silencing complex; however, the molecular mechanism by which the sumoylation machinery is recruited to the transposon loci is poorly understood. Here, we show that the *Drosophila* E3 SUMO-ligase Su(var)2-10 directly binds to the Piwi protein. This interaction is mediated by the SUMO-interacting motif-like (SIM-like) structure in the C-terminal domain of Su(var)2-10. We demonstrated that the SIM-like structure binds to a special region found in the MID domain of the Piwi protein, the structure of which is highly similar to the SIM-binding pocket of SUMO proteins. Abrogation of the Su(var)2-10-binding surface of the Piwi protein resulted in transposon derepression in the ovary of adult flies. Based on our results, we propose a model in which the Piwi protein initiates local sumoylation in the silencing complex by recruiting Su(var)2-10 to the transposon loci.

Introduction

PIWI-interacting RNAs (piRNAs) are small, non-coding RNAs that associate with the PIWI clade of the Argonaute (AGO) protein family. The piRNA pathway functions predominantly in animal gonads and it evolved to silence transposable elements, thereby preserving the genomic integrity of progeny [1–8]. The PIWI proteins are guided to the transposon mRNA by sequence complementarity of their associated piRNAs. In *Drosophila*, the nuclear Piwi/piRNA complexes recognize the nascent transcripts of transposons and induce local heterochromatin formation leading to co-transcriptional silencing. Several factors

required for co-transcriptional silencing have been identified in *Drosophila*; however, the exact mechanism leading to heterochromatin formation is largely unknown. According to a recent model, the Piwi protein recruits a target recognition complex, whose components are specific to the piRNA pathway and include Asterix, Mealstrom, and the SFiNX complex (Panoramix, Nxf2-Nxt1, LC8) [9–16]. The target recognition complex initiates the recruitment of general heterochromatin factors, like SetDB1/Wde histone methyltransferase, which deposits repressive histone methylation marks (H3K9me3) at the target locus.

Abbreviations

AGO, Argonaute; BiFC, bimolecular fluorescence complementation; CTD, C-terminal domain; EGFP, enhanced green fluorescent protein; GSC, germline stem cells; GST, glutathione-S-transferase; HRP, horseradish peroxidase; PIAS, protein inhibitor of activated STAT; piRNAs, PIWI-interacting RNAs; RMSD, root-mean-square deviation; ROI, region of interest; SIM, SUMO Interacting Motif; SUMO, small ubiquitin-like modifiers; YFP, yellow fluorescent protein.

These repressive marks are recognized by effector proteins, such as HP1a, which initiate heterochromatin formation and transcriptional repression [17,18].

A recent study identified several sumoylation targets among the factors involved in the co-transcriptional silencing [19]. Moreover, these sumoylation processes are essential for establishing a link between the Piwi target recognition complex and the heterochromatin machinery [18,20,21]. Sumoylation is a posttranslational modification by which small ubiquitin-like modifiers (SUMOs) are covalently attached to the target proteins. Similar to ubiquitination, sumoylation involves E1 activating, E2 conjugating and E3 ligating enzymes [22–24]. The sumoylated proteins are able to non-covalently bind to SUMO Interacting Motifs (SIMs) of other proteins, which can result in new protein–protein interactions [25]. SIMs are characterized by a hydrophobic core bordered by negatively charged amino acids at their N or C terminus. The hydrophobic core forms a β -strand which interacts with the β -strand of the SIM-binding groove of the SUMO protein. The arrangement of the hydrophobic and acidic residues in SIMs determines the orientation of the SUMO-SIM interaction and can influence the specificity towards distinct SUMO paralogues [26–28].

The E3 SUMO-ligase, Su(var)2-10, associates with the target recognition complex and is essential for Piwi/piRNA-mediated co-transcriptional silencing. According to the recent model, autosumoylation of Su(var)2-10 occurs and the sumoylated Su(var)2-10 recruits the SetDB1/Wde complex through its SIMs [18,20]. Furthermore, the chromatin-bound Panoramix is sumoylated in a Piwi-dependent manner and its SUMO moiety facilitates the interaction with SIMs of Small ovary (Sov) [21]. Sov is a zinc finger protein involved in heterochromatin formation, possibly by stabilizing HP1a on the chromatin [29,30]. Local sumoylation activity of Su(var)2-10 has been proposed to generate “SUMO glue”, which facilitates the assembly of effector complexes by SUMO-SIM interactions [20,21]. However, the first SUMO signal that initiates SUMO glue formation and the molecular mechanism by which the sumoylation machinery is recruited to the site of transposon repression is unknown.

Previous studies have provided evidence that the human AGO2 protein has multiple SIM binding sites through which it directly binds to the SIM motifs of SUMO E3 ligase Nup358. [31,32]. As the structure of the AGO protein family is highly conserved [33], we hypothesized that *Drosophila* Piwi protein also possesses SIM binding sites through which it is able to interact with the SIMs of Su(var)2-10.

Su(var)2-10 is the orthologue of the yeast Siz and human protein inhibitor of activated STAT (PIAS) proteins and belongs to the SP-RING E3 ligase family [34]. The domain composition of the SP-RING protein family is evolutionary conserved from yeast to humans [22,35]. They have a catalytic SP-RING domain and an adjacent C-terminal domain (CTD). The SP-RING domain is responsible for E2 enzyme binding and facilitates SUMO conjugation to the substrate. The SP-RING domain is flanked by N and C-terminal CTD regions, which are connected through a three-stranded β -sheet and form the CTD domain. Structural studies on yeast Siz1 protein revealed that the CTD domain has an embedded SIM-like structure that binds and coordinates the donor SUMO and, thus, is required for the activity of the SP-RING domain [36,37]. The SP-RING ligases also have one or two canonical SIMs in their C-terminal region. The N-terminal region contains a DNA-binding SAP domain and a substrate-binding PINIT motif (Fig. 1A).

Here, we show that the special SIM-like structure in the CTD domain of Su(var)2-10 is able to interact directly with the Piwi protein. We found that the predicted SIM-binding site in the MID domain of the Piwi protein is involved in this interaction and is required for proper transposon silencing in the ovary of *Drosophila*. Based on our results, we propose a model in which the Piwi protein utilizes molecular mimicry of SUMO as an initial SUMO signal to recruit Su(var)2-10 to the site of transposon repression.

Results

Identification of SIMs in *Drosophila* Su(var)2-10

According to the Flybase database, the Su(var)2-10 has 14 possible isoforms. We were able to identify 10 isoforms which are expressed in the ovary (Fig. 1). To predict the domain composition and the possible SIMs of Su(var)2-10 isoforms, we applied *in silico* analyses (Flybase, UniProt, GPS-SUMO) and multiple sequence alignments with Su(var)2-10 orthologues. We found that, all Su(var)2-10 isoforms possess the main functional domains (SAP, PINIT, SpRING) typical to PIAS protein family. The shared region of the isoforms has three possible SIM motifs; however, the PJ and the PL isoforms have one more SIM in their last exon. We selected the PJ isoform for our study.

To experimentally confirm the predicted SUMO binding parts of Su(var)2-10, we performed GST pull-down assays with recombinant GST-tagged fragments of Su(var)2-10 and His-SUMO (Fig. 2). Su(var)2-10 was divided into an N-terminal part (aa 1–278), containing

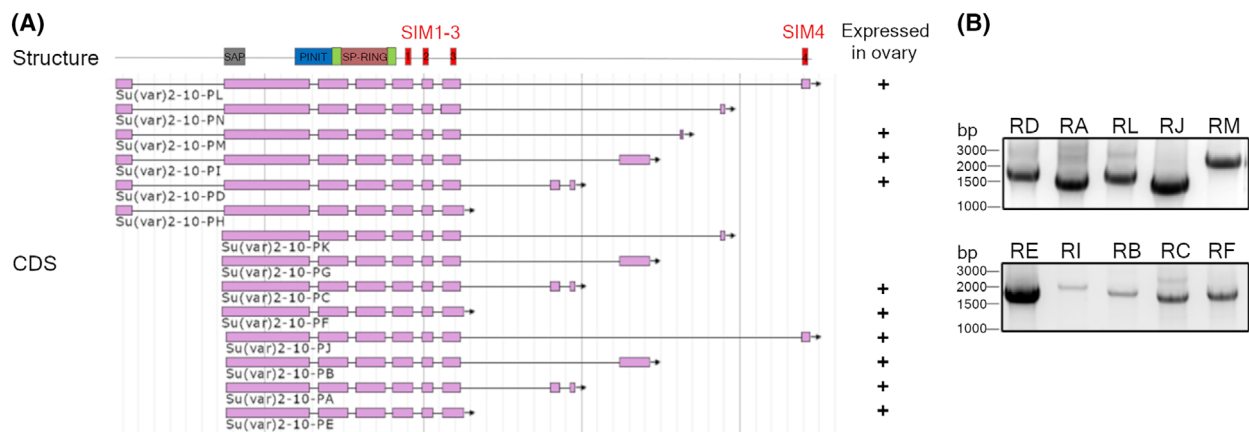


Fig. 1. Identification of Su(var)2-10 isoforms expressed in the ovary. (A) Coding sequence (CDS) of Su(var)2-10 isoforms (adapted from Fly-base using JBrowse). Above is the schematic representation of domain structure and the putative SIMs of isoforms. (B) Expression of Su(var)2-10 isoforms (RA-RM) in the ovary. One representative experiment is shown (from two independent experiments).

the SAP and PINIT domains, a region (aa 278–408), containing the SP-RING and CTD domains, a region (aa 324–378), containing the SP-RING domain without the CTD domain, and a C-terminal part (aa 408–537), containing the predicted SIMs (Fig. 2A). We found that the C-terminal part of Su(var)2-10 has strong SUMO

binding activity, whereas the middle region that included the SP-RING and CTD domains binds to SUMO with a lower affinity. The SP-RING domain itself, without the CTD domain, does not bind SUMO, suggesting that the CTD domain is responsible for the interaction (Fig. 2B).

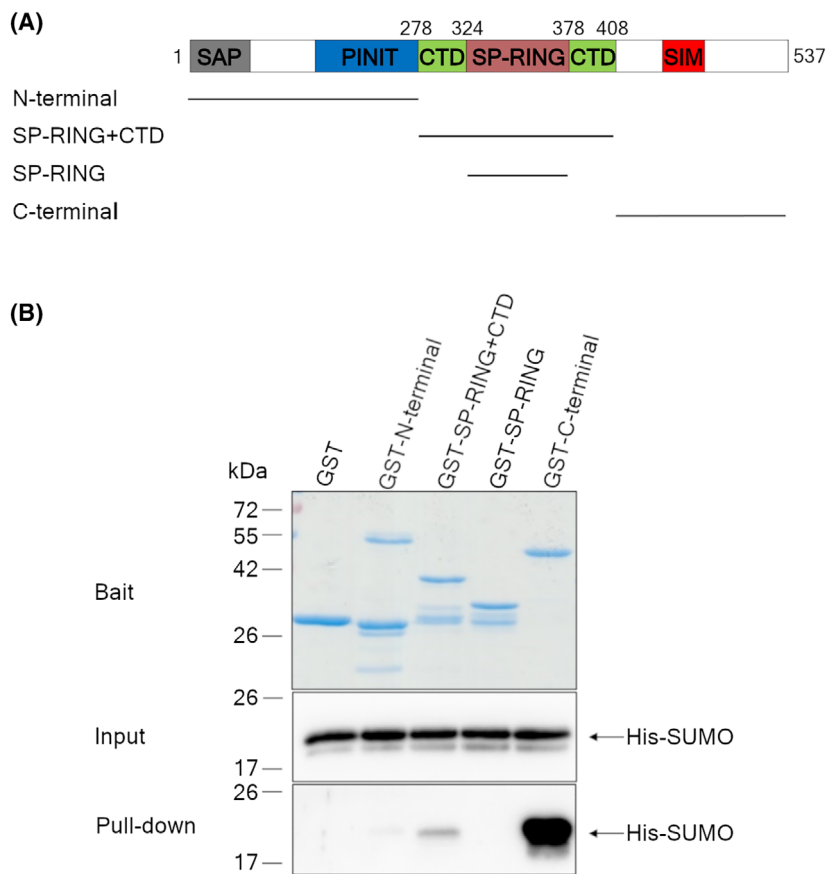


Fig. 2. Identification of SUMO binding regions of *Drosophila* Su(var)2-10. (A) Schematic representation of the domain structure of the Su(var)2-10 PJ isoform. GST-tagged constructs of N-terminal (aa 1–278), SP-RING+CTD (aa 278–408), SP-RING (aa 324–378) and C-terminal (aa 408–537) regions were used for the interaction studies. (B) Pull-down assay using GST or GST-tagged Su(var)2-10 fragments as a bait and His-SUMO as a ligand. The bait proteins were monitored in the pull-down samples by Coomassie blue staining. His-SUMO was detected by western blot using anti-His antibody. One representative experiment is shown (from three independent experiments).

Next, we aimed to identify functional SIMs in the CTD and C-terminal region of Su(var)2-10. In the C-terminal part, four SIMs were predicted by the

GPS-SUMO program: SIM1 (aa 428–432), SIM2 (aa 435–439), SIM3 (aa 465–469) and SIM4 (aa 530–534). Each of these motifs has a canonical hydrophobic core

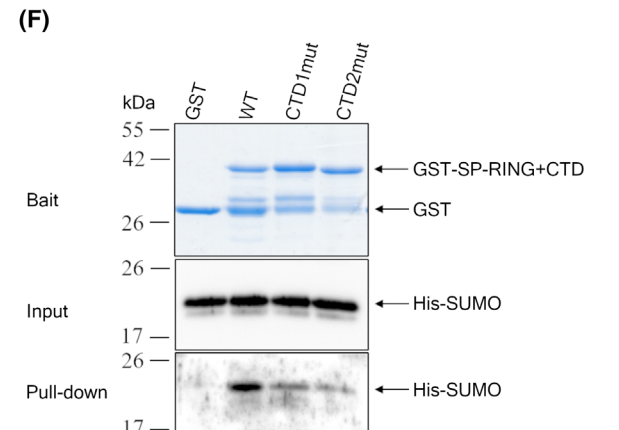
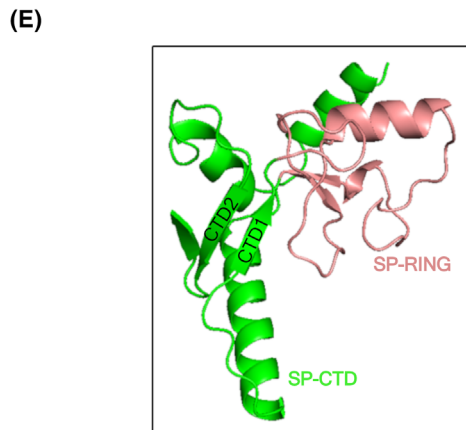
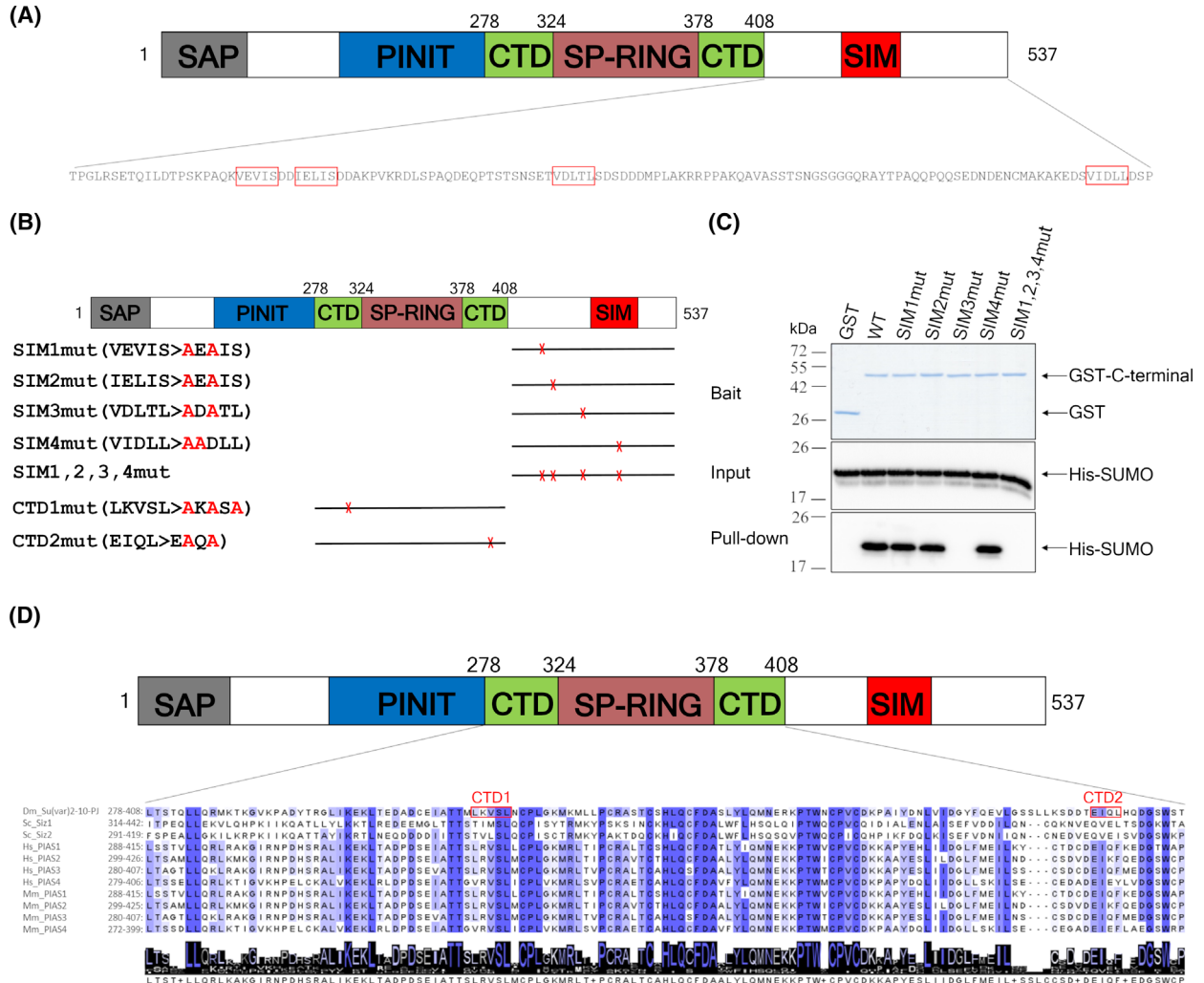


Fig. 3. Identification of SIM motifs in the CTD and C-terminal parts of Su(var)2-10. (A) Amino acid sequence and putative SIM motifs of the C-terminal region. The canonical SIM motifs were predicted by the GPS-SUMO program and their core sequence is framed in red. (B) Schematic representation of mutated constructs used for interaction studies. Amino acid substitutions introduced in predicted SIM motifs are highlighted in red. (C) Pull-down assay using GST-tagged WT and SIM mutant Su(var)2-10 fragments containing the C-terminal region (aa 408–537) as a bait and His-SUMO as a ligand. The GST-tagged bait proteins were monitored in the pull-down samples by Coomassie blue staining. His-SUMO was detected by western blot using anti-His antibody. One representative experiment is shown (from three independent experiments). (D) Amino acid sequence of the SP-RING and CTD domains of the Su(var)2-10 and its budding yeast, human and mouse orthologues. The multiple sequence alignments and the sequence logo were generated by Jalview. The CTD1 and CTD2 sequences are framed in red. (E) The structure of the Su(var)2-10 region containing the SP-RING (salmon) and CTD (green) domains (aa 278–408) was predicted by AlphaFold. The β -strand structures of the CTD1 and CTD2 sequences are labeled. (F) Pull-down assay using GST-tagged WT and SIM mutant Su(var)2-10 fragments containing the SP-RING and CTD domains (aa 278–408) as a bait and His-SUMO as a ligand. The GST-tagged bait proteins were monitored in the pull-down samples by Coomassie blue staining. His-SUMO was detected by western blot using anti-His antibody. One representative experiment is shown (from two independent experiments).

sequence flanked by negatively charged amino acids (Fig. 3A). The predicted SIMs were mutated by exchanging the hydrophobic amino acids to alanine and the effect of the mutations on SUMO binding was examined by GST pull-down assays (Fig. 3B). Individual mutations of SIM1, SIM2 and SIM4 did not affect SUMO binding activity. However, individual mutation of the SIM3 motif and simultaneous mutations of each predicted SIM motif completely abolished SUMO binding in the C-terminal region, indicating that SIM3 is the only functional SIM motif in the C-terminal region of Su(var)2-10 (Fig. 3C).

As the CTD domain does not have predictable, canonical SIMs, we aimed to find a SIM-like structure, based on the fact that the hydrophobic core of SIMs adopts a β -strand conformation.

Based on the AlphaFold prediction of Su(var)2-10-PJ isoform, we selected two β -strand structures in the CTD domain, referred to as CTD1 (aa 319–323) and CTD2 (aa 397–400). These β -strands connect the N and C-terminal parts of the CTD domain by forming an antiparallel β -sheet. (Fig. 3D,E). Mutating the hydrophobic amino acids to alanine in the CTD1 and CTD2 sequences significantly decreased the SUMO binding ability of the CTD domain, indicating that these β -strands contribute to SUMO binding (Fig. 3B, F).

SIM-like structure in the CTD domain of Su(var)2-10 is responsible for Piwi binding

To explore whether Su(var)2-10 is able to bind Piwi directly, we performed interaction studies between the GST-tagged Su(var)2-10 fragments and V5-tagged *Drosophila* Piwi protein expressed in a wheat germ *in vitro* translation system. We found that the fragment containing the SP-RING and CTD domain is the only region of Su(var)2-10 able to interact with

Piwi. The SP-RING domain alone does not have Piwi binding activity, indicating that the interaction is mediated by the CTD domain (Fig. 4A). To investigate whether the predicted SIM-like structure of the CTD domain is responsible for Piwi binding, we analyzed the effect of mutations in the CTD1 and CTD2 sequences in pull-down experiments. Mutations in the CTD2 sequence resulted in decreased Piwi binding, indicating that the SIM-like structure in the CTD domain is necessary for the interaction (Fig. 4B,C).

We aimed to further confirm the pull-down experiments and test the SIM-like activity of the CTD domain in functional assays. For these experiments, we introduced the CTD2 mutations into full-length Su(var)2-10, as these mutations significantly decreased both SUMO and Piwi binding. It was previously shown that Su(var)2-10 has autosumoylation activity [20] and we suggested that the CTD domain could take part in this process by donor SUMO binding. To compare the autosumoylation activity of the wild-type and the CTD2 mutant Su(var)2-10, we applied an *in vitro* sumoylation assay. According to our results, the wild-type Su(var)2-10 was sumoylated in a reaction mixture containing ATP, SUMO, E1 and E2 enzymes, whereas the amounts of SUMO-conjugates decreased in the case of the CTD2 mutant Su(var)2-10. This result indicates that mutations in the CTD2 sequence impair autosumoylation activity of Su(var)2-10, which is possibly due to its decreased donor SUMO binding (Fig. 5A).

To re-evaluate our findings *in vivo*, we expressed GFP-tagged wild-type and CTD2 mutant Su(var)2-10 in *Drosophila* ovaries under the control of the UASp promoter and a germline-specific Gal4 driver. Western blot analysis revealed that the wild-type and the mutant proteins are expressed at comparable levels indicating that the CTD2 mutation does not influence the stability of Su(var)2-10 (Fig. 5B). However, unlike

the wild-type Su(var)2-10 protein, which is localized predominantly in the nucleus, the CTD2 mutant Su(var)2-10 accumulated in the cytoplasm (Fig. 5C). This observation was confirmed by measuring the fluorescence intensity in the nucleus and the cytoplasm. The nuclear/cytoplasmic fluorescence ratio in the wild-type and mutant ovaries were 1.23 and 0.71, respectively (Fig. 5D).

Next, we analyzed the nuclear distribution of wild-type and CTD2 mutant Su(var)2-10. We found that the wild-type protein forms bright dots in the nucleus, which may correspond to SUMO glues in which the

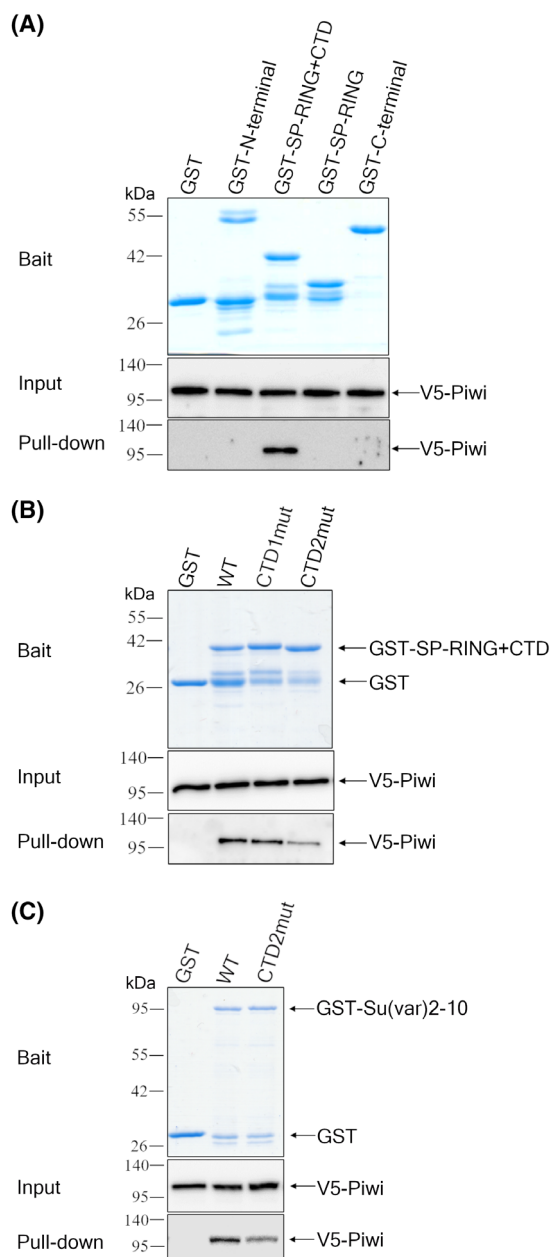


Fig. 4. Identification of Piwi binding sites in Su(var)2-10. (A) Pull-down assay using the same GST-tagged Su(var)2-10 fragments as in Fig. 1. V5-tagged *Drosophila* Piwi expressed in a wheat germ *in vitro* translation system was used as a ligand. The GST-tagged bait proteins were monitored in the pull-down samples by Coomassie blue staining. V5-Piwi was detected by western blot using anti-V5 antibody. (B) Pull-down assay using the GST-tagged WT and SIM mutant Su(var)2-10 fragments containing the SP-RING and CTD domains (aa 278–408) as a bait and V5-Piwi as a ligand. The GST-tagged bait proteins were monitored in the pull-down samples by Coomassie blue staining. V5-Piwi was detected by western blot using anti-V5 antibody. (C) Pull-down assay using the full-length GST-tagged WT and CTD2 mutant Su(var)2-10 protein as a bait and V5-Piwi as a ligand. The GST-tagged bait proteins were monitored in the pull-down samples by Coomassie blue staining. V5-Piwi was detected by western blot using anti-V5 antibody. A–C: One representative experiment is shown (from two independent experiments).

Su(var)2-10 proteins are accumulated. In contrast, the CTD2 mutant Su(var)2-10 has more uniform distribution in the nucleus (Fig. 5C,E).

These experiments confirm that the CTD domain is required for the enzymatic activity of Su(var)2-10. The decreased SUMO binding ability of the CTD2 mutant results in impaired autosumoylation activity. The localization defects of the CTD2 mutant protein most probably due to the lack of SUMO moiety on Su(var)2-10, as sumoylation often influences localization and nucleocytoplasmic transport of substrate proteins [38].

Next, we applied bimolecular fluorescence complementation (BiFC) assay in the ovary of adult flies to confirm the direct interaction between Su(var)2-10 and Piwi proteins *in vivo*. For this experiment, Su(var)2-10 was tagged with the N-terminal part of yellow fluorescent protein (NYFP), while Piwi was tagged with the C-terminal fragment of YFP (CYFP). As a positive control, we used CYFP-tagged SUMO protein. Upon co-expression of Su(var)2-10-NYFP with CYFP-SUMO or CYFP-Piwi transgenes in the ovary, we could detect fluorescence signal in the nuclei of nurse cells (Fig. 6). These results indicate that Su(var)2-10 protein physically interacts with SUMO and Piwi proteins *in vivo*, which lead to reconstitution of the YFP fluorescent protein. CTD2 mutations of Su(var)2-10 resulted in weaker fluorescent signal with SUMO and Piwi proteins. This is most probably due to the mislocalization of the CTD2 mutant Su(var)2-10 protein.

Taken together, these results confirm that the CTD domain of Su(var)2-10 has a functional SIM-like structure similar to its yeast orthologue, Siz1. Mutations of this SIM-like structure resulted in diminished SUMO and Piwi binding, suggesting that Piwi binds to the

CTD domain in a similar manner to SUMO-SIM interactions.

As the wheat germ translation system has no sumoylation activity, moreover, the molecular weight of the translated Piwi protein is equal to the calculated non-sumoylated form, we can exclude the binding of the SIM-like structure of Su(var)2-10 to Piwi through a SUMO moiety.

However, as the PIAS proteins are able to directly interact with their targets, it raises the possibility that the Piwi protein can be sumoylated by Su(var)2-10. To test this possibility, we applied an *in vitro* sumoylation assay using V5-Piwi as a substrate. In a reaction mixture containing ATP, SUMO, E1, E2 enzymes and Su(var)2-10, we could not observe an additional band of higher molecular weight, indicating that Piwi is not modified by sumoylation (Fig. 7). These results confirm that Su(var)2-10 interacts directly with Piwi; however, the Piwi protein is not its sumoylation target.

Piwi binding by the CTD domain of Su(var)2-10 is mediated by SUMO-SIM-like interactions

As the SIM-like structure of the Su(var)2-10 CTD domain is involved in Piwi binding, we hypothesized that it interacts with SIM-binding regions on the Piwi protein, as suggested in the case of human Nup358-AGO2 binding [31]. To identify similar structures on the *Drosophila* Piwi protein, we aligned its structure to human AGO2. Based on this alignment, we identified regions in the MID (aa 511–523) and Piwi (aa 640–648) domains of the Piwi protein which correspond to putative SIM binding sites of AGO2 (Fig. 8A).

Next, we carried out pull-down experiments using the GST-tagged Su(var)2-10 fragment (SP-RING +CTD) as bait and V5-tagged Piwi domains (N, PAZ, MID, Piwi) as ligands. These experiments revealed that each of the four domains of the Piwi protein is able to interact with Su(var)2-10 (Fig. 8B). As the MID domain produced the most prominent binding, it was selected for further investigation. We demonstrated by pull-down experiment that the CTD2 mutation of the Su(var)2-10 fragment (SP-RING +CTD) decreases the interaction with the MID domain (Fig. 8C). This result indicates that the MID domain of Piwi is involved in the binding to the CTD domain of Su(var)2-10.

To test whether the MID domain and SUMO binds to the same site on the CTD domain, we analyzed the SUMO binding and the autosumoylation of Su(var)2-10 in the presence of MID domain. We found that both the SUMO binding capacity in pull-down assay and the auto-sumoylation activity of Su(var)2-10 could be attenuated

by adding increasing amounts of MID domain, indicating that the MID domain was able to compete for the SUMO binding site of CTD domain (Fig. 9).

For further characterization of the CTD:MID interface, we performed *in silico* structural analysis, using the crystal structure of the yeast SP-RING protein, Siz1, complexed with the donor SUMO (32). As the SP-RING and CTD domains of PIAS family proteins are evolutionarily conserved, this allowed us to align this region of Su(var)2-10 (aa 278–408) onto the Siz1 protein [1.365 Å root-mean-square deviation (RMSD) over 120 residues]. Furthermore, the region of the MID domain (aa 511–536) of Piwi protein, including the predicted SIM-binding site, was aligned onto the SIM binding pocket of SUMO protein (aa 32–56) (2.61 Å RMSD over 24 residues) (Fig. 10A).

According to this model, the β -strand of the SIM binding site of MID domain has multiple hydrophobic and polar interactions with the β -strands of CTD1 and CTD2 sequences. Furthermore, the Y517 amino acid in the loop and the positively charged amino acids of the α -helix of SIM binding site of MID domain potentially establish hydrogen bonds and electrostatic interactions with the SIM-like structure of CTD domain (Fig. 10B). Our mutational analysis revealed that deletion of the β -strand of the SIM-binding site of MID domain and Y517A, Y517F, R520A and R526A mutations significantly decreased the CTD:MID interaction (Fig. 10C).

These results indicate that the predicted SIM binding site of MID domain of Piwi protein is involved in the interaction with the CTD domain of Su(var)2-10. Sequence-based structural alignments revealed that this region of the MID domain possesses all of the characteristics of the SIM-binding pocket of SUMO proteins, including a β -strand with hydrophobic and aromatic amino acids followed by a loop and an α -helix with basic residues (Fig. 10D).

Considering together, our results suggest that the MID domain of Piwi protein binds to the CTD domain of Su(var)2-10 by SUMO-SIM-like interactions.

Su(var)2-10 binding surface of Piwi protein is required for transposon silencing in the ovary of adult flies

In order to investigate the biological significance of the identified binding surface, we introduced the Y517A, R520A double mutation into the full-length Piwi protein and analyzed its effect in *Drosophila*. For this study, we used the rescue system described by Stein *et al.* [39]. We generated transgenic flies expressing wild-type or mutant Piwi protein under the control of

the UASp promoter and PiwiGal4 driver on a *Piwi* null background. The hatching rate of eggs laid by flies expressing wild-type or Y517A, R520A mutant Piwi was similar, indicating that the mutant rescue construct restored the developmental defects and

sterility on a *Piwi* null background (Fig. 11A). The expression pattern of the wild-type and the mutant Piwi protein was identical and nuclear localization of the mutant Piwi protein indicates that the Y517A, R520A mutations do not affect the piRNA binding

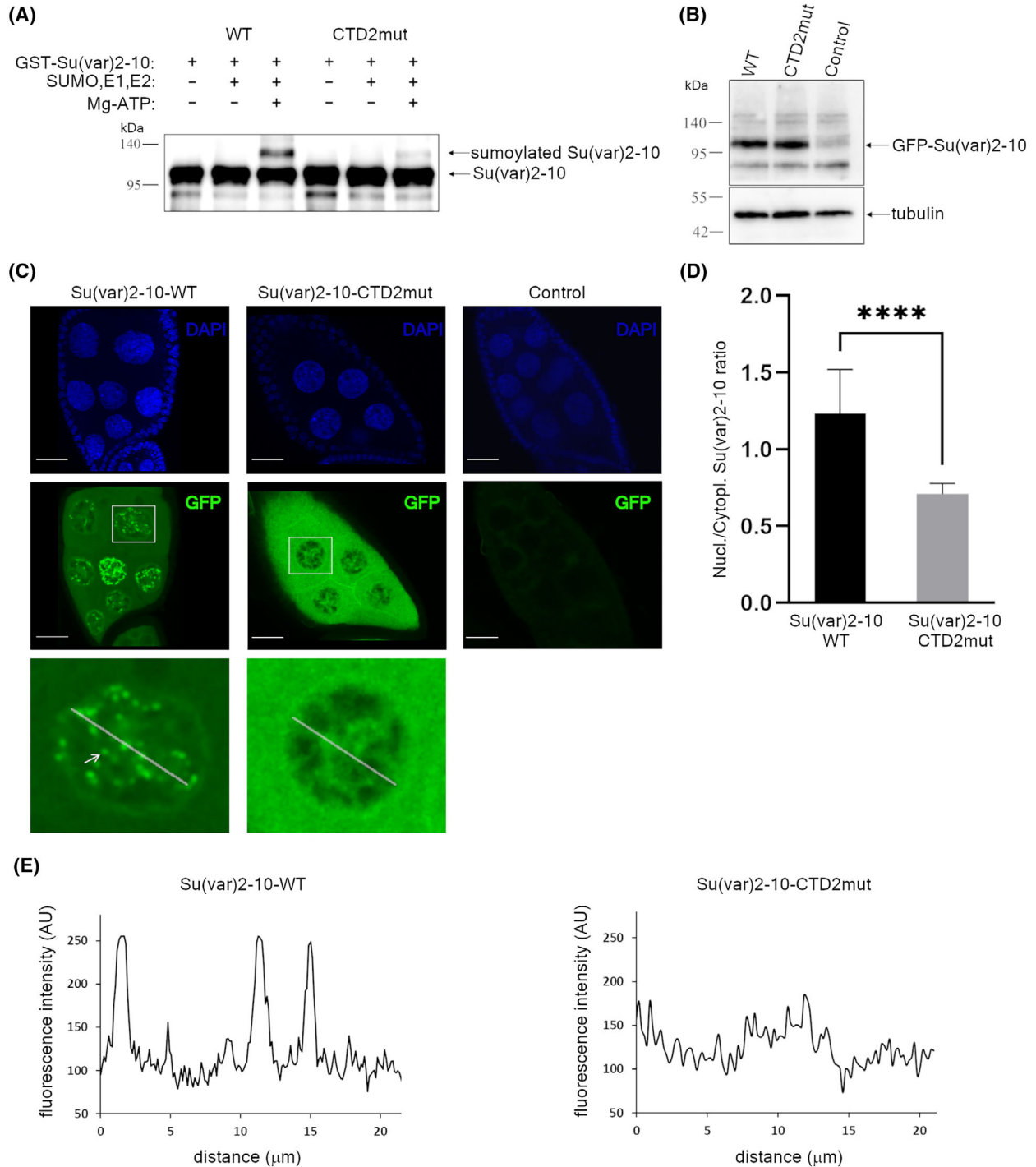


Fig. 5. Functional analysis of the SIM-like structure of Su(var)2-10. (A) Autosumoylation of the WT and CTD2 mutant Su(var)2-10. GST-tagged Su(var)2-10 proteins were incubated with SUMO, E1 and E2 enzymes in the presence or absence of ATP. Su(var)2-10 proteins were detected by western blot using anti-GST antibody. One representative experiment is shown (from three independent experiments). (B) Western blot analysis of GFP-Su(var)2-10 protein in the ovaries of WT, CTD2 mutant and control adult flies using anti-GFP antibody. β -tubulin served as a loading control. One representative experiment is shown (from two independent experiments). (C) *In vivo* localization of WT and CTD2 mutant Su(var)2-10. GFP-tagged Su(var)2-10 was expressed in *Drosophila* egg chambers under the control of UASp promoter and nanosGal4. The tagged Su(var)2-10 protein is green. DAPI labels the nuclei (blue). w^{1118} flies were used as negative control. Scale bar represents 20 μ m. Bottom is the enlargement of WT and CTD2 mutant nucleus (indicated by white squares). Arrow shows nuclear dot in the WT egg chamber. One representative image is shown (from 10 to 10 ovarioles). (D) Quantification of nuclear/cytoplasmic fluorescence intensity ratio of the WT and CTD2 mutant Su(var)2-10 proteins in egg chambers using IMAGEJ software. Data were compared with unpaired *t* test, *****P*-value < 0.0001. Error bars represent standard deviation ($n = 37$ WT and $n = 37$ CTD2 mutant). (E) Measurement of fluorescent intensity in the WT and CTD2 mutant nucleus using IMAGEJ software. Plot profiles were generated along the white lines (indicated in C). One representative experiment is shown (from three independent experiments).

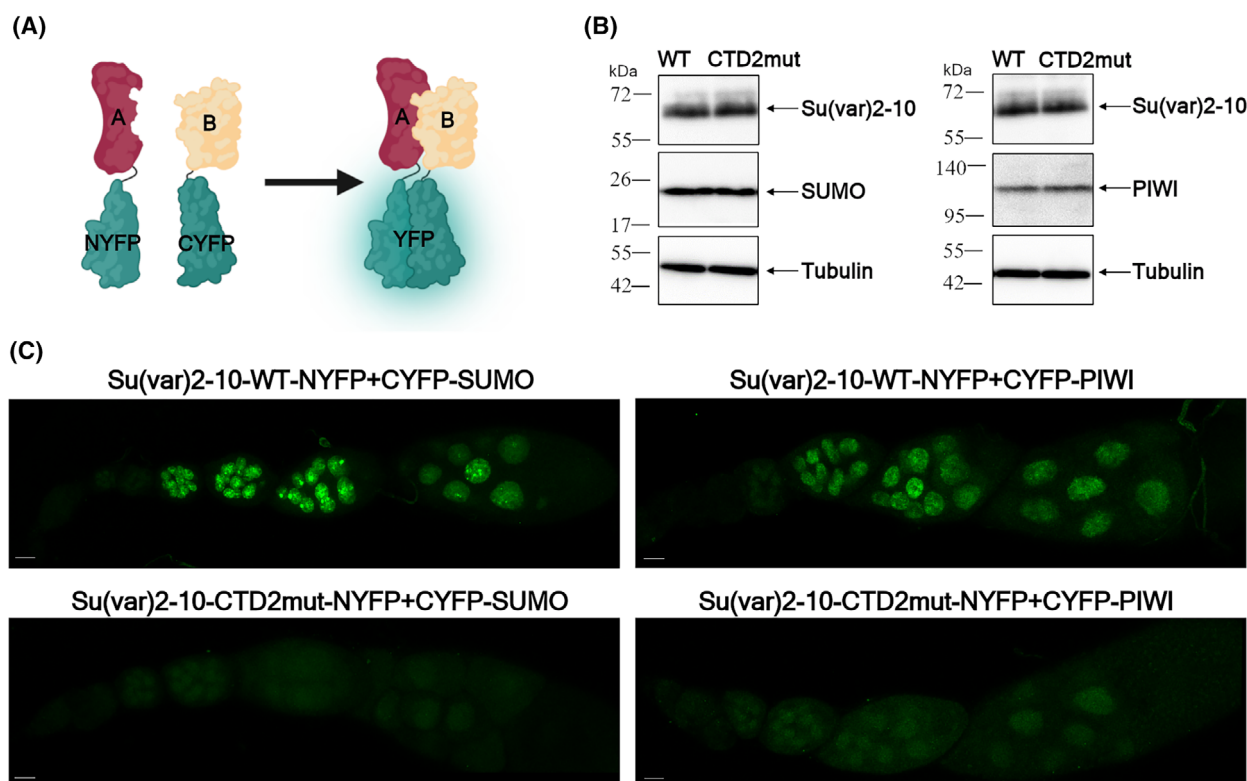


Fig. 6. BiFC assay of Su(var)2-10 interaction with SUMO and Piwi in the adult ovary. (A) Schematic representation of the BiFC assay. Figure was created with BioRender.com. (B, C) WT and CTD2 mutant Su(var)2-10 were tagged with the N-terminal part of YFP and Myc tag. SUMO and Piwi proteins were tagged with the C-terminal part of YFP and V5 tag. Transgenic proteins were expressed in the ovary under the control of UASp promoter and maternal-tubulin Gal4 driver. (B) Expression levels of transgenic proteins in the ovary were analyzed by western blot. Anti-V5 antibody was used for analysis of CYFP-V5-SUMO and CYFP-V5-Piwi proteins. Anti-Su(var)2-10 antibody was used for analysis of WT and mutant Su(var)2-10-Myc-NYFP proteins. β -tubulin served as a loading control. One representative experiment is shown (from two independent experiments). (C) Specific interactions were visualized by green fluorescence in live ovarioles. Scale bar represents 20 μ m. One representative image is shown (from 10 to 10 ovarioles).

ability of the protein (Fig. 11B). Germaria of flies with wild-type and mutant rescue construct contained proper number of germline stem cells with single spermatosomes and differentiating cystocytes with elongated

fusomes, indicating that the Y517A, R520A mutations do not influence the early germ cell development (Fig. 11B). However, double strand breaks were accumulated in the germaria and the early egg chambers of

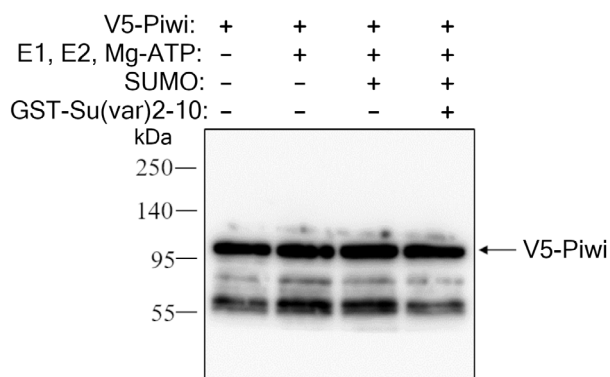


Fig. 7. Sumoylation assay of *Drosophila* Piwi protein. V5-tagged *Drosophila* Piwi was expressed in a wheat germ *in vitro* translation system and incubated with E1, E2 enzymes and ATP in the presence or absence of SUMO and Su(var)2-10. V5-Piwi was detected by western blot using anti-V5 antibody. One representative experiment is shown (from two independent experiments).

the mutant ovaries, compared to the Wild type, where the double strand breaks are restricted to the meiotic region of the germarium (Fig. 11C,D).

Next, we investigated whether decreased Su(var)2-10 binding caused by Y517A, R520A mutations influence Piwi-mediated transposon silencing. To compare the silencing effect of the wild-type and mutant transgenic Piwi, we performed real-time PCR analyses to measure the transcript levels of selected transposons in the ovary of adult flies. Our results revealed that the investigated transposable elements were de-repressed more than 4-fold in the mutant ovary compared to the wild-type control, with the exception of *roo*, whose transcription is not regulated by the Piwi/piRNA system in the adult ovary (Fig. 11E) [40,41].

These results are consistent with our pull-down experiments and indicate that the SIM-binding site in the MID domain of Piwi is important for transposon silencing. However, the upregulation of transposons was relatively low in comparison to other studies depleting the Piwi protein [41–43]. This can be explained by the fact that the Y517A, R520A mutations did not completely abolish the Su(var)2-10 binding capacity of the MID domain (Fig. 10C).

Discussion

Sumoylation plays an essential role in piRNA-mediated co-transcriptional silencing of transposable elements in *Drosophila*. However, the molecular mechanism of the initial recruitment of sumoylation machinery by the Piwi/piRNA complex is poorly understood [20,21]. In this study, we demonstrated that the SUMO-ligase Su(var)2-10 directly binds to the

Piwi protein. This interaction is mediated by the SIM-like structure in the CTD domain of Su(var)2-10. We found that the SIM-like structure is able to interact with the predicted SIM binding site in the MID domain of Piwi. This SIM-binding site shows high structural similarity to the SIM-binding pocket of SUMO proteins. Moreover, modeling the CTD:MID binding interface revealed that the structural basis for the interaction highly resembles that observed between the CTD domain of yeast Siz1 and the SUMO protein [36,37]. This result supports the previous finding that the AGO protein family possesses regions with SIM-binding ability [31,32].

However, we found that the *Drosophila* Piwi protein interacts only with the SIM-like structure of the CTD domain and fails to bind to the canonical SIM motif at the C-terminal end of Su(var)2-10. This suggests that the SIM-binding sites of the Piwi protein are specialized to interact with the CTD domain, which is found exclusively in the SP-RING protein family. Therefore, we suggest that this unique SUMO-SIM-like interaction ensures specificity towards Su(var)2-10 binding and prevents the recruitment of other SIM-containing proteins that are not involved in TE repression.

Although the MID domain produced the strongest interaction with Su(var)2-10 in the pull-down assay, the N, PAZ and Piwi domains also showed Su(var)2-10 binding ability. According to our structural analysis, the Piwi domain also possesses a putative SIM binding site; however, we could not identify similar structures in the N and PAZ domains. This suggests that the Piwi protein utilizes additional binding surfaces beyond the SUMO-SIM-like interactions, which may further increase the specificity of Su(var)2-10 binding. The importance of the other three domains in Su(var)2-10 binding is supported by *in vivo* studies, as abrogating the Su(var)2-10 binding interface of the MID domain of Piwi does not influence fertility and viability of flies and causes only mild upregulation of transposons. Based on these observations, we suggest that a single Piwi protein is able to simultaneously recruit several Su(var)2-10 proteins to the transposon locus.

According to our results, Piwi binding to the CTD domain interferes with donor SUMO binding and attenuates the sumoylation efficiency of Su(var)2-10. Furthermore, Piwi was not sumoylated by Su(var)2-10 in the *in vitro* sumoylation assay, indicating that Piwi does not bind to Su(var)2-10 as a potential substrate. Therefore, it seems that Piwi functions only as a binding platform for Su(var)2-10. We hypothesize that after localization to the transposon locus, Su(var)2-10 dissociates from Piwi to exert its sumoylation activity in the silencing complex. Alternatively, the Piwi-bound

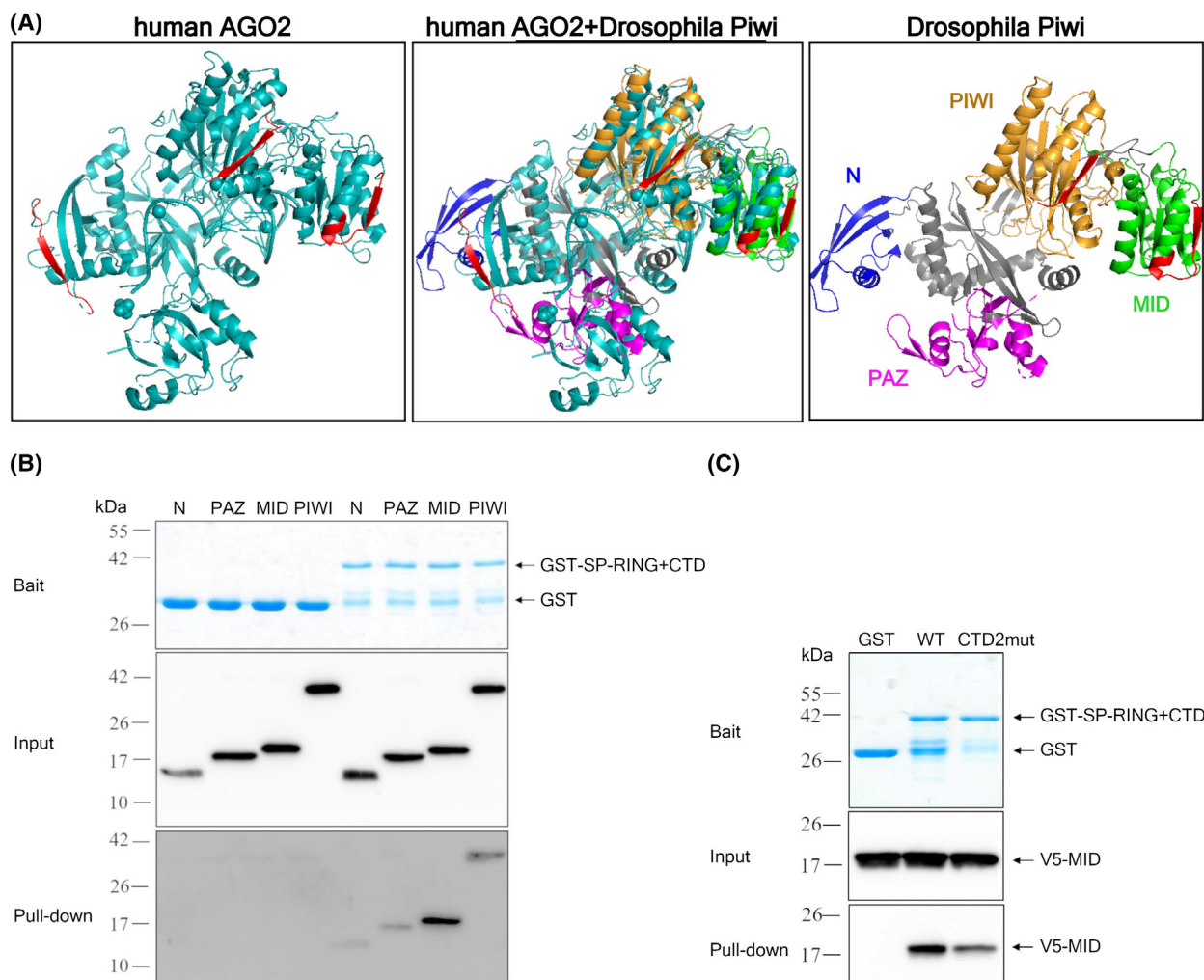


Fig. 8. Identification of Su(var)2-10 binding regions in the Piwi protein. (A) Structural alignment of the human AGO2 (PDB ID: 4W5O) to the *Drosophila* Piwi protein (PDB ID: 6KR6) was performed using PyMOL. Predicted SIM binding sites on human AGO2 (aa 110–120; 490–500; 620–630) and *Drosophila* Piwi (aa 511–523; 640–648) are colored in red. (B) Interaction study between the middle Su(var)2-10 fragment (containing the SP-RING and CTD domains; aa 278–408) and the N (aa 114–186), PAZ (aa 264–372), MID (aa 471–602) and Piwi (aa 603–843) domains of Piwi protein. The GST-tagged Su(var)2-10 fragment was used as a bait and the V5-tagged Piwi domains were used as ligands in a pull-down assay. V5-tagged Piwi domains were expressed in a wheat germ *in vitro* translation system and were detected by western blot in the pull-down samples using anti-V5 antibody. The GST-tagged bait proteins were monitored by Coomassie blue staining. One representative experiment is shown (from three independent experiments). (C) Pull-down assay using the GST-tagged WT and CTD2 mutant Su(var)2-10 fragments containing the SP-RING and CTD domains (aa 278–408) as a bait and V5-tagged MID domain as a ligand. The GST-tagged bait proteins were monitored in the pull-down samples by Coomassie blue staining. V5-MID was detected by western blot using anti-V5 antibody. One representative experiment is shown (from two independent experiments).

Su(var)2-10 operates as an adaptor for the E2 SUMO-conjugase Ubc9. A similar mechanism has been proposed in yeast, where the SUMO-charged Ubc9 is bound to chromatin via the SAP domain of Siz1 and Siz2 ligases. Given a specific trigger (e.g. mitosis or DNA damage), the preassembled protein complexes are recruited to the chromatin and their sumoylation is initiated by Ubc9 alone. The SUMO moieties then recruit Siz ligases through their C-terminal SIMs

which induces a sumoylation wave. This leads to the formation of SUMO glue in which the protein–protein interactions are stabilized by multiple SUMO-SIM interactions [44,45].

Protein group sumoylation and subsequent SUMO glue formation can be also found in nuclear assemblies, such as PML nuclear bodies or nuclear splicing speckles [24,46,47]. As sumoylation enzymes are largely promiscuous, their specificity is often spatially

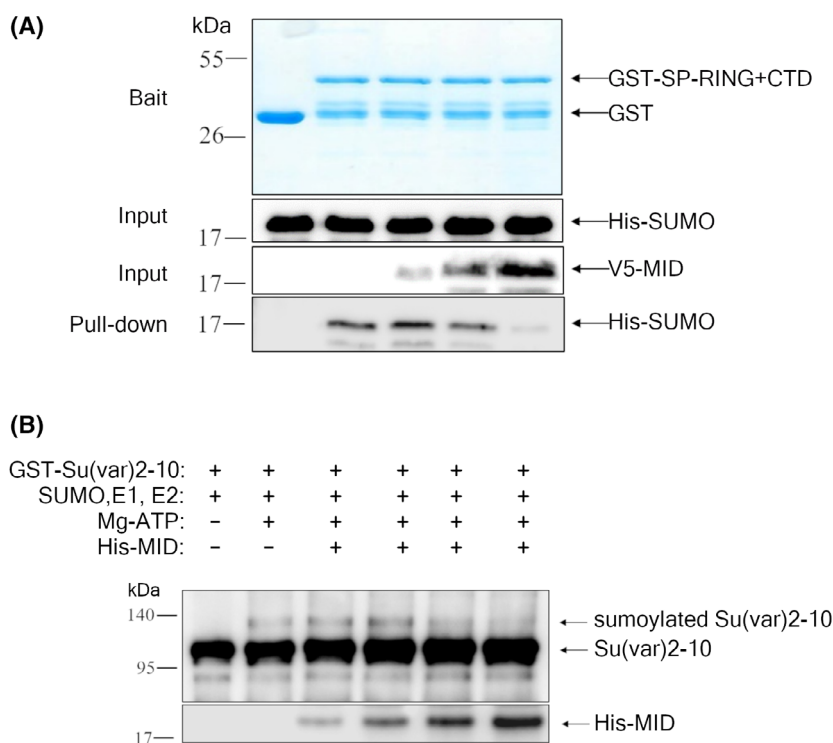


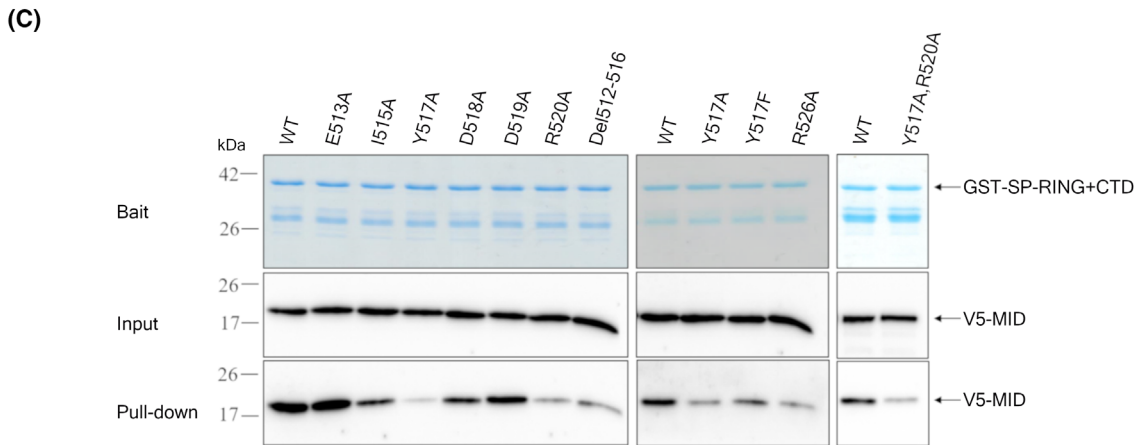
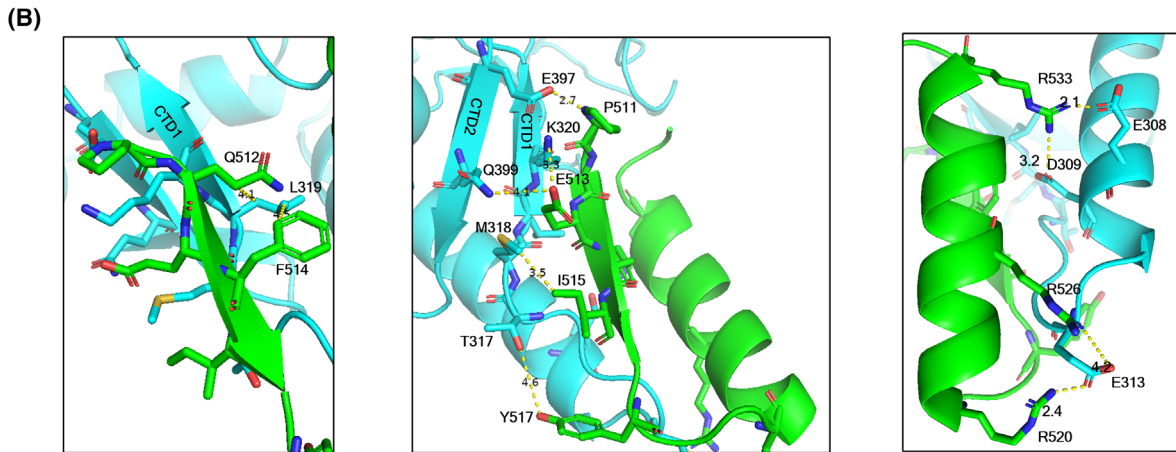
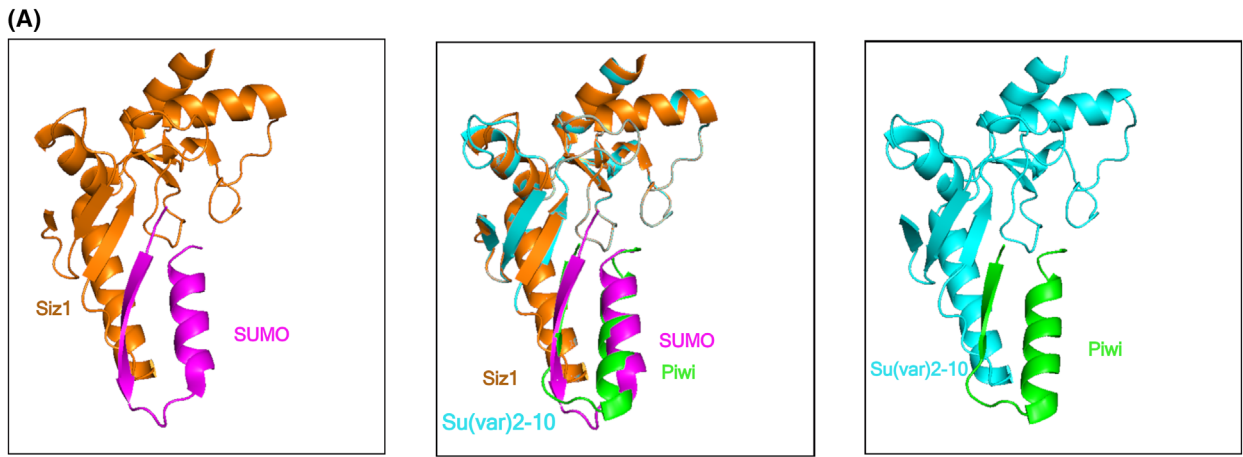
Fig. 9. MID domain of Piwi protein competes with SUMO binding of Su(var)2-10. (A) Pull-down assay of SP-RING+CTD fragment of Su(var)2-10 and SUMO proteins in the presence of increasing amounts of MID domain of Piwi protein. The GST-tagged Su(var)2-10 fragments were monitored in the pull-down samples by Coomassie blue staining. His-SUMO and V5-MID proteins were detected by western blot using anti-His and anti-V5 antibody. One representative experiment is shown (from three independent experiments). (B) GST-tagged Su(var)2-10 protein was incubated with increasing amounts of purified His-MID protein in a sumoylation assay containing SUMO, E1, E2 enzymes and Mg-ATP. Reaction mixture without Mg-ATP was used as a negative control. Su(var)2-10 and MID domain proteins were detected by western blot using anti-GST or anti-His antibody. One representative experiment is shown (from two independent experiments).

regulated and requires only close proximity to their substrates.

Based on our study, we propose a model in which the Piwi protein initiates local sumoylation at the transposon loci by co-recruitment of the sumoylation machinery and the target recognition complex. Sumoylation facilitates the assembly of the target recognition complex by SUMO-SIM interactions. As the nascent

transposon transcripts bind multiple piRNA/Piwi simultaneously, moreover the Piwi protein possesses multiple Su(var)2-10 binding sites, this can concentrate the sumoylation machinery at the site of transcription. The elevated levels of SUMO moieties then recruit general heterochromatin factors through SUMO-SIM interactions and induce SUMO glue formation leading to transcriptional repression of transposons.

Fig. 10. Analysis of the CTD:MID binding surface. (A) Structural model of the CTD:MID binding interface. Structural alignments of the SP-RING + CTD region of Su(var)2-10 (cyan) and yeast Siz1 (orange), and the SIM-binding pocket of the MID domain of Piwi protein (green) and the yeast SUMO protein (purple) were performed by PyMOL using the crystal structure of the budding yeast Siz1 protein complexed with the donor SUMO (PDB ID: 5JNE). The SP-RING+CTD region of Su(var)2-10 (aa 278–408) was predicted by AlphaFold. (B) Putative interactions (dashed yellow lines) between the CTD (cyan) and MID (green) domains. The interacting residues are shown in stick representation. (C) Mutational analysis of the MID domain of Piwi protein. Pull-down assay using GST-tagged Su(var)2-10 fragment containing the SP-RING and CTD domains (aa 278–408) as a bait and WT and mutant V5-tagged MID domains as a ligand. The GST-tagged bait proteins were monitored in the pull-down samples by Coomassie blue staining. V5-MID proteins were detected by western blot using anti-V5 antibody. One representative experiment is shown (from three independent experiments). (D) Structure based sequence alignment of the SIM binding pocket of the MID domain and budding yeast, *Drosophila* and human SUMO orthologues. R520, R526, R533 amino acids of the MID domain and the corresponding basic residues on the SUMO proteins are highlighted by red. β -strand structures are underlined, α -helix structures are underlined by wavy line. Sequences were obtained from UniProt database: *S. cerevisiae* (Q12306), *D. melanogaster* (O97102), human SUMO1 (P63165), human SUMO2 (P61956). Sequence alignment was generated by JALVIEW.



(D)

```

MID      : 512-QEFLIYDDRRTGTYVRAMDDCVRSDP-536
Sc_SMT3  : 33-SEIFFKIKKTPLPLRRLMEAFAKRQG-57
Dm_SUMO  : 23-AVVQFKIKKHTPPLRKLMNAYCDRAG-47
Hs_SUMO1 : 32-SEIHFVKVMTTHLKKLKESYCQRQG-56
Hs_SUMO2 : 28-SVVQFKIKRHTPLSKLMKAYCERQG-51
    
```

Materials and methods

Drosophila stocks

Drosophila stocks were maintained at 25 °C on standard medium. UASp-EGFP-Su(var)2-10-WT and CTD2mut transgenes were integrated into the attP86 landing site (BDSC #24749) and were driven by nosGal4:VP16 (BDSC

#4937). UASp-V5-Piwi-WT and UASp-V5-Piwi-Y517; R520A transgenes were integrated into the attP86 landing site (BDSC #24749) and were driven by [Piwi] > Gal4 (BDSC #83079). The [Piwi] > Gal4 flies express Gal4 instead of Piwi from the *Piwi*-promoter and are homozygous sterile [39]. For the rescue experiments, [Piwi] > Gal4/[Piwi] > Gal4; UASp-V5-Piwi-WT/+ and [Piwi] > Gal4/[Piwi] > Gal4; UASp-V5-Piwi-Y517; R520A/+ flies were generated.

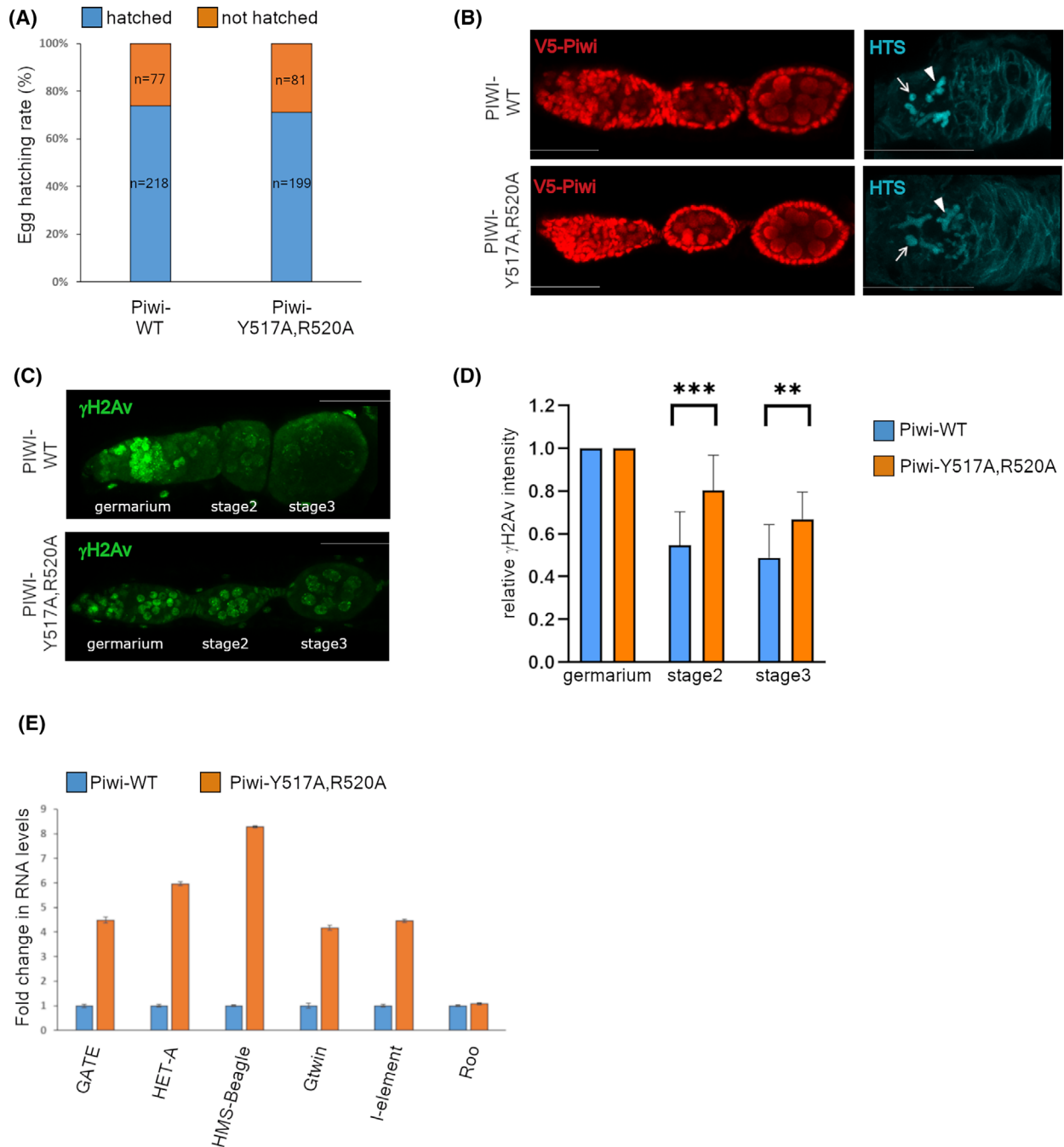


Fig. 11. *In vivo* analysis of Su(var)2-10 binding surface of Piwi protein. Rescue experiment on *Piwi* null background (flies expressing Gal4 instead of Piwi under the control of the endogenous Piwi-promoter [39]) with UASp-V5-Piwi-WT and UASp-V5-Piwi-Y517A, R520A rescue constructs. (A) Hatching rate of eggs laid by females expressing WT or Y517A, R520A mutant Piwi proteins. (B) Immunostaining of the WT and Y517A, R520A mutant adult ovaries. Piwi protein was visualized using anti-V5 antibody (red). Spectrosomes (arrow) and fusomes (arrow-head) are labeled with anti-HTS (blue). Scale bar represents 20 μ m. One representative image is shown (from 13 WT and 15 mutant ovaries). (C, D) Quantification of the double strand breaks in the WT and Y517A, R520A mutant adult ovaries. (C) Double strand breaks were visualized by anti- γ H2Av antibody (green). Scale bar represents 20 μ m. One representative image is shown (from 12 WT and 12 mutant ovaries). (D) Intensity of the γ H2Av staining in the germarium and early egg chambers was measured by IMAGEJ software. Intensity of the γ H2Av staining in the stage2 and stage3 egg chambers was normalized to the intensity measured in the germarium. The relative γ H2Av ratio of the WT and Y517A, R520A mutant ovaries was compared with unpaired *t* test, *P*-value ** = 0.0048; *P*-value *** = 0.0007. Error bars represent standard deviation (*n* = 12 WT and *n* = 12 Y517A, R520A mutant ovaries). (E) RT-qPCR measurement of the indicated transposable elements in the ovary of 3-day-old flies. Expression levels were normalized to the rp49 internal control mRNA. Data were expressed as fold changes relative to levels measured in the ovary of flies expressing V5-Piwi-WT transgene. Error bars represent standard deviation (*n* = 2).

Table 1. Primers used for identification of Su(var)2-10 isoforms.

Isoform	Forward primer (5'–3')	Reverse primer (5'–3')
Su(var)2-10-RA	CGAGAACGCCATGTTTGAGC	GAGCTCTCTGGCTTGGGTTT
Su(var)2-10-RB	CGAGAACGCCATGTTTGAGC	ACGGGCCAATATAGGGACCA
Su(var)2-10-RC	CTGCATAAAGCCGACAAGG	GAGCTCTCTGGCTTGGGTTT
Su(var)2-10-RD	CCCAGGCCAAATGCAAACGAG	CCTTGAGCTCTCTGGCTTGG
Su(var)2-10-RE	CGAGAACGCCATGTTTGAGC	GAGCTCTCTGGCTTGGGTTT
Su(var)2-10-RF	CTGCATAAAGCCGACAAGG	CGTGGTTGAGTCAGTGTGGA
Su(var)2-10-RI	CCCAGGCCAAATGCAAACGAG	ACGGGCCAATATAGGGACCA
Su(var)2-10-RJ	CGAGAACGCCATGTTTGAGC	CCTTGCGGCGGCGATTATG
Su(var)2-10-RL	CCCAGGCCAAATGCAAACGAG	CCTTGCGGCGGCGATTATG
Su(var)2-10-RM	CCCAGGCCAAATGCAAACGAG	CACGGGACGTAAGCAAAGTG

The UASp-CYFP-V5-Piwi and UASp-CYFP-V5-SUMO transgenes were integrated into the attP2 landing site (Cambridge, UK, #13–18), the UASp-Su(var)2-10-WT-Myc-NYFP and UASp-Su(var)2-10-CTD2mut-Myc-NYFP transgenes were integrated into the attP40 landing site (Cambridge, UK, #13–20). The transgenes were driven by maternal-tubulin Gal4 (BDSC #7063).

Identification of Su(var)2-10 isoforms

Total RNA was isolated from 10 pairs of ovaries of 3-day-old adult females using the RNeasy RNA tissue Miniprep System (Promega, Madison, WI, USA, Z6111). 1 μ g RNA was reverse-transcribed with oligo dT primers using the First Strand cDNA Synthesis kit (Thermo Scientific, Waltham, MA, USA, K1612). For PCR reactions we used isoform specific primers (Table 1). PCR products were sequenced by Eurofins.

Plasmid construction

The UASp-EGFP-Suvar-PJ plasmid was generated via the following consecutive cloning steps: First, EGFP was PCR-amplified from the pTagNG-EGFP plasmid [48] using

pTagNG-EGFP-fwd and pTagNG-EGFP-rev primers. The PCR product was digested with NotI-BamHI restriction enzymes and cloned into the pUASp-K10attB plasmid [49]. Next, the coding region of the PJ isoform of Su(var)2-10 was PCR-amplified from cDNA prepared from the Oregon-R fly strain (BDSC # 5). The PCR product was cloned into the UASp-EGFP-K10-attb plasmid by a SLIC reaction [50] using Su(var)-PJ-UASp-fwd and Su(var)-PJ-UASp-rev primers.

For the generation of the pGEX-Su(var)2-10-PJ plasmid, the coding region of the PJ isoform of Su(var)2-10 was PCR-amplified from the UASp-EGFP-Suvar-PJ plasmid. The PCR product was digested with NotI and BamHI restriction enzymes and cloned into the pGEX-6P-1 plasmid (Addgene, Watertown, MA, USA, 27-4597-01) using Su(var)-PJ-pGEX-fwd and Su(var)-PJ-pGEX-rev primers.

For the generation of the GST-tagged Su(var)2-10 fragments, the appropriate regions of Su(var)2-10 were PCR-amplified from the pGEX-Su(var)2-10-PJ plasmid and were cloned into the pGEX-6P-1 (GE Healthcare, Chicago, IL, USA) plasmid with a SLIC reaction using the following primers: N-terminal part (1–834 nucleotides): Su(var)-PJ-N-term-fwd and Su(var)-PJ-N-term-rev primers. SP-RING+CTD part (835–1224 nucleotides): Su

(var)-PJ-SP-RING+CTD-fwd and Su(var)-PJ-SP-RING+CTD-rev primers. SP-RING part (969–1134 nucleotides): Su(var)-PJ-SP-RING-fwd and Su(var)-PJ-SP-RING-rev primers. C-terminal part (1225–1611 nucleotides): Su(var)-PJ-C-term-fwd and Su(var)-PJ-C-term-rev primers.

For the generation of pET16b-His-SUMO, the coding region of *Drosophila* SUMO was PCR-amplified from the pAc-GFP-dSUMO plasmid (Addgene, 85696). The PCR product, generated by making use of pAc-SUMO-fwd and pAc-SUMO-rev primers, was digested with NdeI and BamHI restriction enzymes and cloned into the pET16b plasmid (Novagen, 69662-3).

To generate the UASp-V5-dPiwi plasmid, the coding region of *Drosophila* Piwi was PCR-amplified from cDNA prepared from the Oregon fly strain using dPiwi-UASp-fwd and dPiwi-UASp-rev primers. The N-terminal V5-tag was introduced by the forward primer. The PCR product was digested with NotI and XbaI restriction enzymes and cloned into the UASp-K10-attB plasmid.

For the BiFC assay, the Su(var)2-10 was tagged at the C-terminal end with the N-terminal fragment of YFP (NYFP), while the Piwi and SUMO proteins were tagged at the N-terminal end with the C-terminal fragment of YFP (CYFP). NYFP and CYFP fragments were PCR-amplified from split YFP tagging vectors (kind gift of Sven Bogdan, Münster, Germany) [51] and cloned into the UASp-Su(var)2-10-WT, UASp-Su(var)2-10-CTD2mut, UASp-V5-dPiwi or UASp-V5-SUMO plasmids by SLIC reaction.

For the generation of the pHY22-V5-FL-Piwi plasmid, the coding region of dPiwi was PCR-amplified from the UASp-V5-dPiwi plasmid using dPiwi-pHY22-fwd and dPiwi-pHY22-rev primers. The PCR product was digested with HindIII and XbaI restriction enzymes and cloned into the pPHY22 plasmid.

For the generation of V5-tagged Piwi domains, the appropriate regions of Piwi were PCR-amplified from the pPHY22-V5-dPiwi plasmid by the following pairs of primers: N domain (340–558 nucleotides): dPiwi-N-fwd and dPiwi-N-rev primers, PAZ domain (790–1116 nucleotides): dPiwi-PAZ-fwd and dPiwi-PAZ-rev primers, MID domain (1411–1806 nucleotides): dPiwi-MID-fwd and Piwi-MID-rev primers, Piwi domain (1807–2529 nucleotides): dPiwi-Piwi-fwd and dPiwi-Piwi-rev primers. PCR products were cloned into the pPHY22 plasmid with SLIC reactions.

For generation of His-tagged MID domain, the coding region of MID domain was PCR amplified from the pPHY22-V5-dPiwi plasmid using His-MID-fwd and His-MID-rev primers. The PCR product was digested with NdeI and BamHI restriction enzymes and cloned into the pET16b plasmid (Novagen, Darmstadt, Germany, 69662-3).

Mutations were introduced into the plasmids using the QuikChange Lightning Site-directed Mutagenesis Kit (Agilent Technologies, Santa Clara, CA, USA) according to the manufacturer's instruction.

Primer sequences used in PCR reactions are listed in Table 2.

Protein production and purification

For production of GST or GST-tagged proteins, pGEX-6P-1 constructs were transformed in *E. coli* strain BL21 and induced by 0.5 mM IPTG at 18 °C O/N. Cells were lysed in lysis buffer [50 mM Tris-HCl, pH 7.4, 5 mM DTT, 50 mM NaCl, 5 mM EDTA, 10% glycerol, 25× protease inhibitor cocktail (Roche, Basel, Switzerland, 11697498001)] using sonication. The lysates were supplemented with 1% Triton-X-100 and incubated on ice for 30 min. Glutathione Sepharose 4B (GE Healthcare) beads were equilibrated using five bead volumes of lysis buffer and were incubated with lysates for 2 h at 4 °C with end-over-end rotation. After three washes with washing buffer (50 mM Tris-HCl, pH 7.4, 5 mM DTT, 50 mM NaCl, 5 mM MgCl₂, 10 mM KCl, 5% glycerol), the proteins were eluted with elution buffer (50 mM Tris-HCl, pH8, 5 mM DTT, 50 mM NaCl, 5 mM MgCl₂, 10 mM KCl, 5% glycerol, 25 mM reduced L-Glutathione). Elution buffer was exchanged for storing buffer (50 mM Tris-HCl, pH7.4, 150 mM NaCl, 1 mM DTT, 5% glycerol) using PD-midiTrap G-25 column (GE Healthcare). Protein solutions were concentrated using 3 kDa MWCO Amicon Ultra-4 Centrifugal Filter (Millipore, Burlington, MA, USA) and stored at –80 °C.

For production of the His-tagged SUMO protein and His-tagged MID domain, the pET16b-His-SUMO and pET16b-His-MID plasmids were transformed in *E. coli* strain BL21(DE3) SixPack [52] and induced by 0.5 mM IPTG at 18 °C O/N. Cells were lysed in lysis buffer [100 mM NaH₂PO₄ × H₂O pH 8, 150 mM NaCl, 5 mM Imidazol, 7× EDTA-free protease inhibitor cocktail (Roche, 04693132001)] using sonication. The lysate was supplemented with 1% Triton-X-100 and incubated on ice for 30 min. Talon Metal Affinity Resin (Takara BIO, Göteborg, Sweden) beads were equilibrated using five bead volumes of lysis buffer and was incubated with lysate for 2 h at 4 °C with end-over-end rotation. After three washes with washing buffer (100 mM NaH₂PO₄ × H₂O pH 8, 300 mM NaCl, 20 mM Imidazol), His-SUMO was eluted with elution buffer (100 mM NaH₂PO₄ × H₂O pH 8, 300 mM NaCl, 300 mM Imidazol). Elution buffer was exchanged for storing buffer (50 mM Tris-HCl, pH 7.4, 150 mM NaCl, 1 mM DTT, 5% glycerol) using a PD-midiTrap G-25 column (GE Healthcare). The protein solution was concentrated using a 3 kDa MWCO Amicon Ultra-4 Centrifugal Filter (Millipore) and stored at –80 °C.

The V5-tagged full-length Piwi and Piwi domains were produced with the TNT® SP6 High-Yield Wheat Germ Protein Expression System (Promega, L3260) according to the manufacturer's instruction using 8.5 µg pPHY22 constructs in 50 µL reaction volume.

Table 2. Primers used for cloning.

Primer name	Sequence (5'–3')
pTagNG-EGFP-fwd	AAAGCGGCCGCGCCACCATGGTCAGTAAGGGAGAAGA
pTagNG-EGFP-rev	TTTGGATCCTGCCCCAGCACCAGCCCGCGCCCTGCACCCCTGTACAACCTCATCCATGC
Su(var)-PJ-UASp-fwd	CTGGTGTGGGGCAGGATCCGTGCAGATGCTTCGAGTGGTC
Su(var)-PJ-UASp-rev	ACGTTTCGAGGTCGACTCTAGATTATGGCGAATCTAGAAGATCAATTACGG
Su(var)-PJ-pGEX-fwd	AAAGGATCCGTGCAGATGCTTCGAGTGGTC
Su(var)-PJ-pGEX-rev	TTTGCAGGCCGCTTATGGCGAATCTAGAAGATCAATTACGG
Su(var)-PJ-N-term-fwd	TCCAGGGGCCCTGGGATCCGGCGGTGGAGGCTCTGTGCAGATGCTTCGAGTGGTC
Su(var)-PJ-N-term-rev	GTCAGTCACGATGCGGCCGCTTAGAGCTTCTTTACCAGGTATACGG
Su(var)-PJ-SP-RING+CTD-fwd	TCCAGGGGCCCTGGGATCCGGCGGTGGAGGCTCTACCTCAACACAGCTTTTGCAGC
Su(var)-PJ-SP-RING+CTD-rev	GTCAGTCACGATGCGGCCGCTTATGTGCTCCAAGATCCATCCTGAT
Su(var)-PJ-SP-RING-fwd	TCCAGGGGCCCTGGGATCCGGCGGTGGAGGCTCTAACGCTCCGTTGGGCAAGATG
Su(var)-PJ-SP-RING-rev	GTCAGTCACGATGCGGCCGCTTATGTGCTCCAAGATCCATCCTGAT
Su(var)-PJ-C-term-fwd	TCCAGGGGCCCTGGGATCCGGCGGTGGAGGCTCTCCAGGACTACGGAGCGAGAC
Su(var)-PJ-C-term-rev	GTCAGTCACGATGCGGCCGCTTATGGCGAATCTAGAAGATCAATTACGG
pAc-SUMO-fwd	AAACATATGTCTGACGAAAAGAAGGGAGG
pAc-SUMO-rev	TTTGGATCCTTATGGAGCGCCACCAGTCT
dPiwi-UASp-fwd	AAAGCGGCCGCGCCACCATGGGTAAGCCTATCCCTAACCCCTCCTCGGTCTCGATTCTAC GGGCGGTGGAAGATCTGCTGATGATCAGGGACGTGG
dPiwi-UASp-rev	TTTTCTAGATTATAGATAATAAAAACCTTCTTTTCGAGCGCG
dPiwi-pHY22-fwd	AAAAAGCTTACCACCATGGGTAAGCCTATCCCTAACC
dPiwi-pHY22-rev	TTTTCTAGATTATAGATAATAAAAACCTTCTTTTCGAGCGCG
dPiwi-N-fwd	TCGATTCTACGGGCGGTGGAAGATCTATCGTTTATTATCACGTGGAG
dPiwi-N-rev	GCTCGCCCGGGGATCGATCCTCTAGATTATATGAATCCAACGAACTTTATGG
dPiwi-PAZ-fwd	TCGATTCTACGGGCGGTGGAAGATCTATCTACGACATAATGCGACGTTG
dPiwi-PAZ-rev	GCTCGCCCGGGGATCGATCCTCTAGATTACCCAGTCACTCGGCAGA
dPiwi-MID-fwd	TCGATTCTACGGGCGGTGGAAGATCTCCGAGCGATGGCCCTCGAT
dPiwi-MID-rev	GCTCGCCCGGGGATCGATCCTCTAGATTATTTCGATCATCCAGGGTGTATATC
dPiwi-Piwi-fwd	TCGATTCTACGGGCGGTGGAAGATCTCTACCCTTGTCCGGACTGAT
dPiwi-Piwi-rev	GCTCGCCCGGGGATCGATCCTCTAGATTATAGATAATAAAAACCTTCTTTTCGAGCG
His-MID-fwd	CCATATCGAAGGTCGTCATATGCCGAGCGATGGCCCTCGATC
His-MID-rev	GCTTTGTAGCAGCCGGATCCTTATTCGATCATCCAGGGTGTATATCCC

GST pull-down assay

10 µg GST or GST-tagged proteins were bound to 20 µL Glutathione Sepharose 4B beads (GE Healthcare) and incubated with 3 µg purified His-SUMO or 10 µL wheat germ reaction mixture containing V5-Piwi for 2 h at 4 °C in binding buffer (50 mM HEPES pH 7.5, 150 mM NaCl, 2 mM MgCl₂, 1 mM EGTA, 1 mM DTT, 0.1% TritonX-100, 0.5 mg·mL⁻¹ BSA). After washing three times with the same buffer, the proteins were eluted by incubating the beads with 2× SDS/PAGE buffer for 5 min at 95 °C. The GST-tagged bait proteins were visualized with Coomassie blue staining, the His-SUMO and V5-Piwi proteins were detected by western blot.

In vitro sumoylation assay

In vitro sumoylation assays were performed using the SUMOylation Assay Kit (Abcam, Cambridge, UK, ab139470) according to the manufacturer's instruction. For

analysis of autosumoylation activity of WT and CTD2 mutant Su(var)2-10 protein, 2–2 µg GST-tagged Su(var)2-10 protein was incubated in 20 µL reaction volume for 1 h at 37 °C. To test the effect of the MID domain, increasing amounts of purified His-MID protein (150–900 ng) were added into the autosumoylation assay of WT Su(var)2-10 protein.

To test the sumoylation of Piwi protein by Su(var)2-10, the V5-Piwi was expressed in wheat germ *in vitro* translation system, then 2 µL of reaction mixture and 2 µg GST-Su(var)2-10 protein was incubated in 20 µL sumoylation assay for 1 h at 37 °C.

Western blot

Proteins were separated by SDS-polyacrylamide gel electrophoresis and subsequently transferred onto PVDF membranes (Millipore) for immunoblotting. Membranes were incubated in rabbit anti-GFP (1 : 2000, Life Technologies,

Carlsbad, CA, USA, A11122), mouse anti- β -tubulin (1 : 300, DSHB, Iowa City, IA, USA), mouse anti-V5 (1 : 5000, Invitrogen, Waltham, MA, USA, 46-0705) and mouse anti-Su(var)2-10 (1 : 2000, kind gift of Julius Brennecke, Vienna, Austria [21]) primary antibodies at 4 °C overnight. Secondary antibodies were horseradish peroxidase (HRP)-conjugated anti-rabbit IgG (1 : 6000, Sigma, Burlington, MA, USA) or HRP-conjugated anti-mouse IgG (1 : 5000, Sigma) antibodies. HRP-conjugated anti-His (1 : 10 000, Sigma-Aldrich, A7058-1VL) and anti-GST (1 : 10 000, Millipore, 16-209) antibodies were applied for 1 h at room temperature. Immunocomplexes were visualized with enhanced chemiluminescence reactions (Millipore) using the UVITEC Alliance Q9 system.

Immunostaining, microscopy, and fluorescence intensity measurement

Ovaries were dissected from 3-day-old adult females and fixed in PBS with 4% formaldehyde for 20 min. The samples were incubated overnight at 4 °C with anti-V5 (mouse, 1 : 400, Invitrogen, 46-0705), anti-HTS (mouse, 1 : 20, 1B1, DSHB) or anti- γ H2Av (mouse, 1 : 50, UNC93-5.2.1, DSHB) primary antibodies. Anti-mouse Alexa Fluor 546 (1 : 600, Life Technologies) secondary antibody and DAPI (200 ng·mL⁻¹, Sigma) was used for 1 h at 25 °C. To examine the expression pattern of WT and CTD2 mutant GFP-tagged Su(var)2-10 protein, the samples were stained with DAPI (200 ng·mL⁻¹, Sigma) for 1 h at 25 °C. Stained ovaries were mounted in Fluoromount-G medium (Southern-Biotech, Birmingham, AL, USA, #0100-01). All micrographs were taken using a ZEISS LSM800 confocal laser scanning microscope. The fluorescence intensity of the GFP-tagged Su(var)2-10 protein and the γ H2Av staining was measured by IMAGEJ software [53]. Region of interests were outlined by hand. Statistical tests were performed with GraphPad Prism. The distribution of WT and mutant GFP-tagged Su(var)2-10 protein inside the nucleus was measured by IMAGEJ software using Plot Profile tool.

Quantitative real-time PCR

Total RNA was isolated from 10 pairs of ovaries of 3-day-old adult females using the RNeasy RNA tissue Miniprep System (Promega, Z6111). 1 μ g RNA was reverse-transcribed with random primers using the First Strand cDNA Synthesis kit (Thermo Scientific, K1612). qPCRs were performed in duplicate using the Maxima SYBR Green/ROX qPCR Kit (Thermo Scientific, K0222). Reactions without reverse-transcriptase were used as negative controls. Amplification and signal detection were performed using the Rotor-Gene Q System (Qiagen, Venlo, the Netherlands). Denaturation at 95 °C for 10 min, was followed by 40 thermocycles (65 °C, 15 s, and 60 °C, 1 min). Gene expression was quantified using the

Table 3. Primers used for RT-qPCR.

Primer name	Sequence (5'–3')
RP49-fwd	CCGCTTCAAGGGACAGTATCTG
RP49-rev	ATCTCGCCCGCAGTAAACGC
GATE-fwd	GTCAGCCTTTAAGCTTTCGATG
GATE-rev	CAGCATGATGTCCCTGTACTTG
HET-A-fwd	CGCGCGGAACCCATCTTCAGA
HET-A-rev	CGCCGCGAGTCGTTTGGTGAGT
HMS-Beagle-fwd	AATGCCCTTGTGCGGACACGA
HMS-Beagle-rev	TGATGAAACACATTACCAGAACCCTTGA
Gtwin-fwd	TTCGCACAAGCGATGATAAG
Gtwin-rev	GATTGTTGTACGGCGACCTT
l-element-fwd	GACCAAATAAAAATAATACGACTT
l-element-rev	AACTAATTGCTGGCTTGTATG
Roo-fwd	CAGTCACTTGAGATCGTTCCC
Roo-rev	GTAAATAGTCCCCGCCCTTATCG

comparative CT method ($\Delta\Delta$ CT method). Threshold cycle (CT) values were determined using the Rotor-Gene Q Series software. Expression levels of target genes were first normalized to the Rp49 internal control gene (Δ CT) and then to expression levels measured in the WT ovary ($\Delta\Delta$ CT). Results were expressed as fold changes calculated with the formula $2^{-\Delta\Delta$ CT}. Primers used in PCR reactions are listed in Table 3.

In silico analysis

The SIMs of Su(var)2-10 were predicted by the GPS-SUMO program: <http://sumosp.biocuckoo.org/> [54]. Sequences and domain compositions of *Drosophila* Piwi (CG6122) and Su(var)2-10-PJ isoform (CG8068) were obtained from Flybase: <https://flybase.org/> and UniProt: <https://www.uniprot.org/> databases. Multiple sequence alignments and sequence logo of Su(var)2-10 orthologues were generated by JALVIEW. <https://www.jalview.org/>.

AlphaFold structure of Su(var)2-10-J isoform was obtained from the Uniprot database. (AF-A0A0B4JD03-F1-model_v3) [55].

Structure of the *Drosophila* Piwi (6KR6), human AGO2 (4W5O), and yeast Siz1 complexed with the donor SUMO, Ubc9 and PCNA (5JNE) were downloaded from Protein Data Bank (PDB). Structural alignments were performed by PyMOL: <https://pymol.org/2/>.

Acknowledgements

We thank Margit Ugrainé Szathmári for valuable technical assistance, László Sipos and *Drosophila* Injection Facility of the BRC, Jennifer Tusz for English proof-reading. We are thankful to Beat Suter for providing the pUASp-K10attB plasmid and Astrid D. Haase for [Piwi] > Gal4 fly stocks and Julius Brennecke for the anti-Su(var)2-10 antibody. This research was funded

by the National Research, Development and Innovation Office (K132384, National Laboratory for Biotechnology 2022-2.1.1-NL-2022-00008 to ME and PD124446 to MB). MB was supported by János Bolyai Fellowship of Hungarian Academy of Sciences (BO/00599/17) and ÚNKP New National Excellence Program of the Ministry of Human Capacities of Hungary (UNKP-19-4-SZTE-5). BGV was supported by the National Research, Development and Innovation Office (K135231, K146890, FK137867, VEKOP-2.3.2-16-2017-00013, NKP-2018-1.2.1-NKP-2018-00005), and the TKP2021-EGA-02 grant, implemented with the support provided by the Ministry for Innovation and Technology of Hungary from the National Research, Development and Innovation Fund.

Conflict of interest

The authors declare no conflict of interest.

Author contributions

MB: conceptualization, formal analysis, methodology, investigation, visualization, funding acquisition, writing—original draft, writing—review and editing; FJ: conceptualization, methodology, writing—review and editing; IK: methodology; ÁG: investigation; BGV: Conceptualization, Writing – review and editing; ME: Conceptualization, Funding acquisition, Project administration, Writing – review and editing.

Peer review

The peer review history for this article is available at <https://www.webofscience.com/api/gateway/wos/peer-review/10.1111/febs.17073>.

Data availability statement

The data that support the findings of this study are available from the corresponding authors (bence.melinda@brc.hu; erdelyi.miklos@brc.hu) upon reasonable request.

References

- Aravin AA, Hannon GJ & Brennecke J (2007) The Piwi-piRNA pathway provides an adaptive defense in the transposon arms race. *Science* **318**, 761–764.
- Chen P & Aravin AA (2021) Transposon-taming piRNAs in the germline: where do they come from? *Mol Cell* **81**, 3884–3885.
- Ninova M & Fejes Tóth K (2020) New players on the piRNA field. *Nat Struct Mol Biol* **27**, 777–779.
- Luteijn MJ & Ketting RF (2013) Piwi-interacting RNAs: from generation to transgenerational epigenetics. *Nat Rev Genet* **14**, 523–534.
- Czech B, Munafò M, Ciabrelli F, Eastwood EL, Fabry MH, Kneuss E & Hannon GJ (2018) piRNA-guided genome defense: from biogenesis to silencing. *Annu Rev Genet* **52**, 131–157.
- Pillai RS & Chuma S (2012) piRNAs and their involvement in male germline development in mice: piRNAs and their involvement in male germline. *Dev Growth Differ* **54**, 78–92.
- Parhad SS & Theurkauf WE (2019) Rapid evolution and conserved function of the piRNA pathway. *Open Biol* **9**, 180181.
- Ryazansky S, Radion E, Mironova A, Akulenko N, Abramov Y, Morgunova V, Kordyukova MY, Olovnikov I & Kalmykova A (2017) Natural variation of piRNA expression affects immunity to transposable elements. *PLoS Genet* **13**, e1006731.
- Zhao K, Cheng S, Miao N, Xu P, Lu X, Zhang Y, Wang M, Ouyang X, Yuan X, Liu W *et al.* (2019) A Pandas complex adapted for piRNA-guided transcriptional silencing and heterochromatin formation. *Nat Cell Biol* **21**, 1261–1272.
- Ohtani H, Iwasaki YW, Shibuya A, Siomi H, Siomi MC & Saito K (2013) DmGTSF1 is necessary for Piwi-piRISC-mediated transcriptional transposon silencing in the *Drosophila* ovary. *Genes Dev* **27**, 1656–1661.
- Eastwood EL, Jara KA, Bornelöv S, Munafò M, Frantzis V, Kneuss E, Barbar EJ, Czech B & Hannon GJ (2021) Dimerisation of the PICTS complex via LC8/Cut-up drives co-transcriptional transposon silencing in *Drosophila*. *eLife* **10**, e65557.
- Schnabl J, Wang J, Hohmann U, Gehre M, Batki J, Andreev VI, Purkhauser K, Fasching N, Duchek P, Novatchkova M *et al.* (2021) Molecular principles of Piwi-mediated cotranscriptional silencing through the dimeric SFiNX complex. *Genes Dev* **35**, 392–409.
- Murano K, Iwasaki YW, Ishizu H, Mashiko A, Shibuya A, Kondo S, Adachi S, Suzuki S, Saito K, Natsume T *et al.* (2019) Nuclear RNA export factor variant initiates piRNA-guided co-transcriptional silencing. *EMBO J* **38**, e102870.
- Yu Y, Gu J, Jin Y, Luo Y, Preall JB, Ma J, Czech B & Hannon GJ (2015) Panoramix enforces piRNA-dependent cotranscriptional silencing. *Science* **350**, 339–342.
- Batki J, Schnabl J, Wang J, Handler D, Andreev VI, Stieger CE, Novatchkova M, Lampersberger L, Kauneckaite K, Xie W *et al.* (2019) The nascent RNA binding complex SFiNX licenses piRNA-guided heterochromatin formation. *Nat Struct Mol Biol* **26**, 720–731.
- Sienski G, Dönertas D & Brennecke J (2012) Transcriptional silencing of transposons by Piwi and

- Maelstrom and its impact on chromatin state and gene expression. *Cell* **151**, 964–980.
- 17 Le Thomas A, Rogers AK, Webster A, Marinov GK, Liao SE, Perkins EM, Hur JK, Aravin AA & Tóth KF (2013) Piwi induces piRNA-guided transcriptional silencing and establishment of a repressive chromatin state. *Genes Dev* **27**, 390–399.
 - 18 Ninova M, Fejes Tóth K & Aravin AA (2019) The control of gene expression and cell identity by H3K9 trimethylation. *Development* **146**, dev181180.
 - 19 Ninova M, Holmes H, Lomenick B, Fejes Tóth K & Aravin AA (2023) Pervasive SUMOylation of heterochromatin and piRNA pathway proteins. *Cell Genomics* **3**, 100329.
 - 20 Ninova M, Chen Y-CA, Godneeva B, Rogers AK, Luo Y, Fejes Tóth K & Aravin AA (2020) Su(var)2-10 and the SUMO pathway link piRNA-guided target recognition to chromatin silencing. *Mol Cell* **77**, 556–570.e6.
 - 21 Andreev VI, Yu C, Wang J, Schnabl J, Tirian L, Gehre M, Handler D, Duchek P, Novatchkova M, Baumgartner L *et al.* (2022) Panoramix SUMOylation on chromatin connects the piRNA pathway to the cellular heterochromatin machinery. *Nat Struct Mol Biol* **29**, 130–142.
 - 22 Pichler A, Fatouros C, Lee H & Eisenhardt N (2017) SUMO conjugation – a mechanistic view. *Biomol Concepts* **8**, 13–36.
 - 23 Flotho A & Melchior F (2013) Sumoylation: a regulatory protein modification in health and disease. *Annu Rev Biochem* **82**, 357–385.
 - 24 Vertegaal ACO (2022) Signalling mechanisms and cellular functions of SUMO. *Nat Rev Mol Cell Biol* **23**, 1–17.
 - 25 Song J, Durrin LK, Wilkinson TA, Krontiris TG & Chen Y (2004) Identification of a SUMO-binding motif that recognizes SUMO-modified proteins. *Proc Natl Acad Sci U S A* **101**, 14373–14378.
 - 26 Lussier-Price M, Masclé XH, Cappadocia L, Kamada R, Sakaguchi K, Wahba HM & Omichinski JG (2020) Characterization of a C-terminal SUMO-interacting motif present in select PIAS-family proteins. *Structure* **28**, 573–585.e5.
 - 27 Hecker C-M, Rabiller M, Haglund K, Bayer P & Dikic I (2006) Specification of SUMO1- and SUMO2-interacting motifs. *J Biol Chem* **281**, 16117–16127.
 - 28 Kerscher O (2007) SUMO junction—what’s your function?: new insights through SUMO-interacting motifs. *EMBO Rep* **8**, 550–555.
 - 29 Jankovics F, Bence M, Sinka R, Faragó A, Bodai L, Pettkó-Szandtner A, Ibrahim K, Takács Z, Szarka-Kovács AB & Erdélyi M (2018) *Drosophila* *small ovary* gene is required for transposon silencing and heterochromatin organisation and ensures germline stem cell maintenance and differentiation. *Development* **145**, dev.170639.
 - 30 Ninova M, Godneeva B, Chen Y-CA, Luo Y, Prakash SJ, Jankovics F, Erdélyi M, Aravin AA & Fejes Tóth K (2020) The SUMO ligase Su(var)2-10 controls hetero- and euchromatic gene expression via establishing H3K9 trimethylation and negative feedback regulation. *Mol Cell* **77**, 571–585.e4.
 - 31 Sahoo MR, Gaikwad S, Khuperkar D, Ashok M, Helen M, Yadav SK, Singh A, Magre I, Deshmukh P, Dhanvijay S *et al.* (2017) Nup358 binds to AGO proteins through its SUMO-interacting motifs and promotes the association of target mRNA with miRISC. *EMBO Rep* **18**, 241–263.
 - 32 Deshmukh P, Markande S, Fandade V, Ramtirtha Y, Madhusudhan MS & Joseph J (2021) The miRISC component AGO2 has multiple binding sites for Nup358 SUMO-interacting motif. *Biochem Biophys Res Commun* **556**, 45–52.
 - 33 Yamaguchi S, Oe A, Nishida KM, Yamashita K, Kajiya A, Hirano S, Matsumoto N, Dohmae N, Ishitani R, Saito K *et al.* (2020) Crystal structure of *Drosophila* Piwi. *Nat Commun* **11**, 858.
 - 34 Hari KL, Cook KR & Karpen GH (2001) The *Drosophila* *Su(var)2-10* locus regulates chromosome structure and function and encodes a member of the PIAS protein family. *Genes Dev* **15**, 1334–1348.
 - 35 Rytinki MM, Kaikkonen S, Pehkonen P, Jääskeläinen T & Palvimo JJ (2009) PIAS proteins: pleiotropic interactors associated with SUMO. *Cell Mol Life Sci* **66**, 3029–3041.
 - 36 Streich FC Jr & Lima CD (2016) Capturing a substrate in an activated RING E3/E2–SUMO complex. *Nature* **536**, 304–308.
 - 37 Yunus AA & Lima CD (2009) Structure of the Siz/PIAS SUMO E3 ligase Siz1 and determinants required for SUMO modification of PCNA. *Mol Cell* **35**, 669–682.
 - 38 Ptak C & Wozniak RW (2017) SUMO and nucleocytoplasmic transport. In *SUMO Regulation of Cellular Processes* (Wilson VG, ed.), pp. 111–126. Springer International Publishing, Cham.
 - 39 Stein CB, Genzor P, Mitra S, Elchert AR, Ipsaro JJ, Benner L, Sobti S, Su Y, Hammell M, Joshua-Tor L *et al.* (2019) Decoding the 5′ nucleotide bias of Piwi-interacting RNAs. *Nat Commun* **10**, 828.
 - 40 Gu T & Elgin SCR (2013) Maternal depletion of Piwi, a component of the RNAi system, impacts heterochromatin formation in *Drosophila*. *PLoS Genet* **9**, e1003780.
 - 41 Fabry MH, Falconio FA, Joud F, Lythgoe EK, Czech B & Hannon GJ (2021) Maternally inherited piRNAs direct transient heterochromatin formation at active transposons during early *drosophila* embryogenesis. *eLife* **10**, e68573.
 - 42 Senti K-A, Jurczak D, Sachidanandam R & Brennecke J (2015) piRNA-guided slicing of

- transposon transcripts enforces their transcriptional silencing via specifying the nuclear piRNA repertoire. *Genes Dev* **29**, 1747–1762.
- 43 Akkouche A, Mugat B, Barckmann B, Varela-Chavez C, Li B, Raffel R, Péliousson A & Chambeyron S (2017) Piwi is required during *Drosophila* embryogenesis to license dual-Strand piRNA clusters for transposon repression in adult ovaries. *Mol Cell* **66**, 411–419.e4.
- 44 Jentsch S & Psakhye I (2013) Control of nuclear activities by substrate-selective and protein-group SUMOylation. *Annu Rev Genet* **47**, 167–186.
- 45 Psakhye I & Jentsch S (2012) Protein group modification and synergy in the SUMO pathway as exemplified in DNA repair. *Cell* **151**, 807–820.
- 46 Keiten-Schmitz J, Röder L, Hornstein E, Müller-McNicoll M & Müller S (2021) SUMO: glue or solvent for phase-separated ribonucleoprotein complexes and molecular condensates? *Front Mol Biosci* **8**, 673038.
- 47 Matunis MJ, Zhang X-D & Ellis NA (2006) SUMO: the glue that binds. *Dev Cell* **11**, 596–597.
- 48 Ejsmont RK, Ahlfeld P, Pozniakovskiy A, Stewart AF, Tomancak P & Sarov M (2012) Recombination-mediated genetic engineering of large genomic DNA transgenes. In *Molecular Methods for Evolutionary Genetics* (Orgogozo V & Rockman MV, eds), pp. 445–458. Humana Press, Totowa, NJ.
- 49 Koch R, Ledermann R, Urwyler O, Heller M & Suter B (2009) Systematic functional analysis of bicaudal-D serine phosphorylation and intragenic suppression of a female sterile allele of BicD. *PLoS One* **4**, e4552.
- 50 Jeong J-Y, Yim H-S, Ryu J-Y, Lee HS, Lee J-H, Seen D-S & Kang SG (2012) One-step sequence- and ligation-independent cloning as a rapid and versatile cloning method for functional genomics studies. *Appl Environ Microbiol* **78**, 5440–5443.
- 51 Gohl C, Banovic D, Grevelhörster A & Bogdan S (2010) WAVE forms hetero- and homo-oligomeric complexes at integrin junctions in *Drosophila* visualized by bimolecular fluorescence complementation. *J Biol Chem* **285**, 40171–40179.
- 52 Lipinszki Z, Vernyik V, Farago N, Sari T, Puskas LG, Blattner FR, Posfai G & Gyorfy Z (2018) Enhancing the translational capacity of *E. coli* by resolving the codon bias. *ACS Synth Biol* **7**, 2656–2664.
- 53 Schneider CA, Rasband WS & Eliceiri KW (2012) NIH image to ImageJ: 25 years of image analysis. *Nat Methods* **9**, 671–675.
- 54 Zhao Q, Xie Y, Zheng Y, Jiang S, Liu W, Mu W, Liu Z, Zhao Y, Xue Y & Ren J (2014) GPS-SUMO: a tool for the prediction of sumoylation sites and SUMO-interaction motifs. *Nucleic Acids Res* **42**, W325–W330.
- 55 Jumper J, Evans R, Pritzel A, Green T, Figurnov M, Ronneberger O, Tunyasuvunakool K, Bates R, Žídek A, Potapenko A *et al.* (2021) Highly accurate protein structure prediction with AlphaFold. *Nature* **596**, 583–589.